



UNIVERSITY COLLEGE LONDON

MENG MECHANICAL ENGINEERING

MECH0074 ENGINEERING IN EXTREME ENVIRONMENTS

TOPIC NOTES

Author:

HD

Module coordinator:

Prof. Ian Eames

February 12, 2023

Contents

List of Figures	3
List of Tables	5
I Extreme Pressure	6
1 Materials, Molecules and Chemistry	7
1.1 Introduction	7
1.1.1 Complexity of the problem at different length scales	7
1.1.2 Why focus on small scales?	8
1.2 Categorisation of matter	10
1.3 Atomistic view of matter	10
1.3.1 Bulk characteristic of materials	10
1.3.2 Newtonian model of matter	11
1.3.3 Vibrational modes and energy	12
1.3.4 Molecular description of material properties	12
1.3.5 Material classification	16
1.4 Kinetic theory of gases	19
1.4.1 Speed of molecules	19
1.4.2 Equations of state of real gases	19
1.5 Chemistry for engineers	21
II Extreme Temperature	22
2 How to Cool Very Hot Surfaces	23
2.1 Introduction	23
2.2 Jet engines	23
2.2.1 Brayton (or Joule) cycle	24
2.2.2 Typical values	25
2.2.3 Material selection	26
2.2.4 Manufacturing process	28
2.2.5 Thermal barrier coating	29
2.2.6 Corrosion processes	32
2.2.7 Cooling through design	33
2.3 Atmospheric re-entry objects	34
2.3.1 Idealised re-entry path	35
2.3.2 Blunt body entry vehicles	36
2.3.3 Shock layer physics	37
2.3.4 Different types of coatings	37
2.3.5 Thermal soak	38
2.3.6 Cooling methods	38

2.4 Conclusions	38
3 Large Spatial and Temporal Variations of Temperature	39
3.1 Introduction	39
3.2 Practical application of heat to a material	40
3.2.1 Welding	40
3.2.2 Friction welding	41
3.2.3 Radiation heating	42
3.2.4 Laser heating	42
3.3 Structural changes in the matter	43
3.3.1 Microstructural changes	43
3.3.2 Macroscopic changes	44
3.4 Soldering, brazing, welding	45
3.5 Rapid changes in temperature	47
3.5.1 Thermal shock	47
3.5.2 Stress criterion	48
3.5.3 Strain criterion	48
3.5.4 Fraction criterion	49
3.5.5 Material selection	50
3.6 Conclusions	51
4 Low temperature environments	52
4.1 Introduction	52
4.2 Engineering applications	54
4.2.1 LNG - liquefied natural gas	54
4.2.2 Cryogenic transport	54
4.3 Thermal bowing	55

List of Figures

1.1	Pressure pulsation in a piping system	7
1.2	Graph to show complexity against scale.	8
1.3	Graph to show complexity against scale.	9
1.4	Example of plasticity from internal grain process level.	9
1.5	Hydrogen embrittlement - plastic deformation / slip	9
1.6	Rust corrosion from grain boundary level.	10
1.7	Ionic bond (electrovalence)	12
1.8	Bond stability.	12
1.9	Covalent bond (covalence). Note the overlap of electron orbit.	13
1.10	Metallic bond (electron cloud).	13
1.11	Secondary bonds. Note: long range attractive force - dipole-dipole interactions. Overlapping electron orbits - repulsive.	14
1.12	Young's modulus from atomic perspective.	15
1.13	Graph to show yield stress ratio for different materials.	16
1.14	Nucleation of crystals.	17
1.15	Stress-strain curve.	18
1.16	Toplogical changes in crystal structure.	19
1.17	Speed of molecules.	19
1.18	Van der Waals.	20
2.1	Jet engine.	23
2.2	Brayton (or Joule) cycle.	24
2.3	Typical temperature values for different stages of cycle in bypass gas-turbine engine.	25
2.4	Efficiencies of various gas-turbine engines.	26
2.5	Usage of different alloys within the engine.	27
2.6	Development of alloys.	27
2.7	Oxidation and corrosion resistance of different alloys.	28
2.8	Temperature resistance of TBCs and CMCs over the years.	29
2.9	Thermal barrier coatings (TBCs).	29
2.10	Thermal barrier coating composition.	30
2.11	Microstructure of TBC.	31
2.12	Failure of TBCs.	32
2.13	Schematic illustration of corrosive molten salts infiltration into the YSZ layer of different TBC coatings.	32
2.14	Cooling holes.	33
2.15	Blade with cooling holes.	33
2.16	Classes of cooling technologies for internal blade cooling.	34
2.17	Idealised re-entry path.	35
2.18	Re-entry path for Earth.	36
2.19	Re-entry path for Earth.	36
2.20	Shapes of entry path.	37
3.1	Heating processes.	40

3.2	Localised heating processes.	40
3.3	Friction welding.	41
3.4	Radiation heating.	42
3.5	Laser heating.	42
3.6	Close-up of laser heating.	43
3.7	Close-up of laser heating.	43
3.8	Effect on microstructure from cold rolling and then annealing.	44
3.9	Influence of localised heating on a weld.	45
3.10	Thermoplastic shrinkage.	46
3.11	Weld shrinkage.	46
3.12	Plate heating.	47
3.13	Rapid changes in temperature characterised.	47
3.14	Thermal shock.	48
3.15	Crack lengths against temperature difference.	49
3.16	Crack lengths , temperature difference, strength and fracture stress.	50
4.1	LNG carrier.	52
4.2	Thermal bowing.	55
4.3	Fixed end beam subjected to a uniform thermal gradient.	55
4.4	Laterally restrained beam subjected to a uniform thermal gradient.	56
4.5	Cross-section of pipe.	57

List of Tables

1.1	Cascade of length scales	7
1.2	Micrograph	8
1.3	Categorisation of matter	10
1.4	Key points on material properties	11
1.5	Comparison between molecular and macroscopic measurements.	15
1.6	Configurations of atoms.	17
2.1	Introduction.	23
2.2	Table to show melting points of various metals used in bypass gas-turbine engines.	25
2.3	Table to show combustion temperatures of various fuels.	25
2.4	Internal blade configurations.	34
3.1	Spatial and temporal heat application.	40
3.2	Welding efficiencies.	45
4.1	Freezing temperatures of various gases.	52
4.2	Tables to show material properties of storage tanks.	53
4.3	Table to show materials used to store different low temperature materials.	54

Part I

Extreme Pressure

Chapter 1

Materials, Molecules and Chemistry

1.1 Introduction

- Macorscopic response of material depends on their microscopic structure
- We need to be able to understand physics from molecular to continuum scales

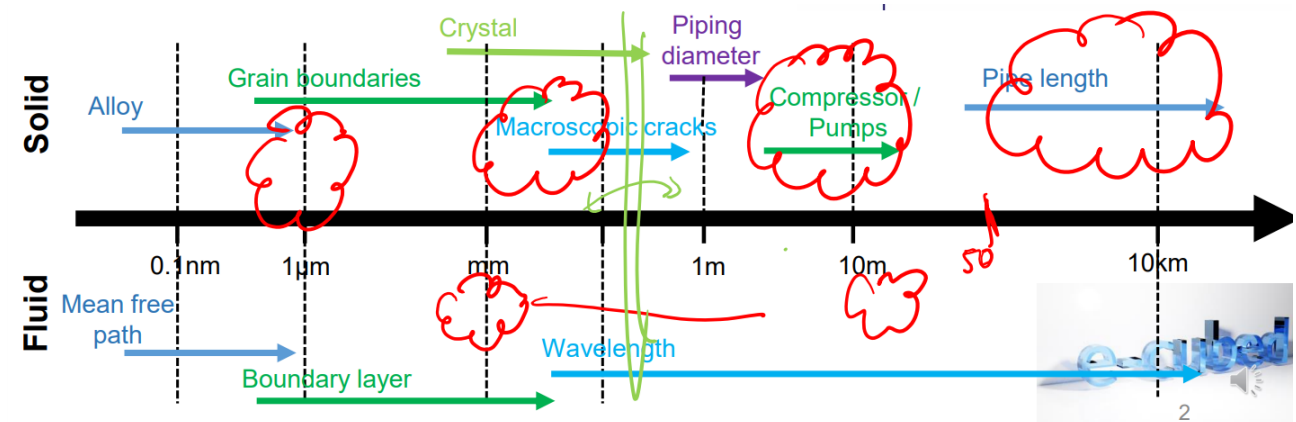


Figure 1.1: Pressure pulsation in a piping system

Cascade of length scales

1.1.1 Compelxity of the problem at different length scales

Complexity of representation changes with the scale.

Molecular	Continuum	Structural
Material is made on this level	Cracks operate on this level	Structures considered at this level
$< 10\mu\text{m}$	$10\mu\text{m} < x < 10\text{ m}$	$> 10\text{ m}$
Short range interactions	Long range interactions	Whole scale interactions
Failure / corrosion / chemistry	Tune model - variables change continuously / smoothly (can account for discontinuous behaviour, e.g. crack)	Long distance interaction - vibration (waves transporting energy)

Table 1.1: Cascade of length scales

Domain	Process
Bulk	Plasticity
Internal boundary	Hydrogen embrittlement - plastic deformation / slip
External boundary	Corrosion - chemistry

Table 1.2: Micrograph

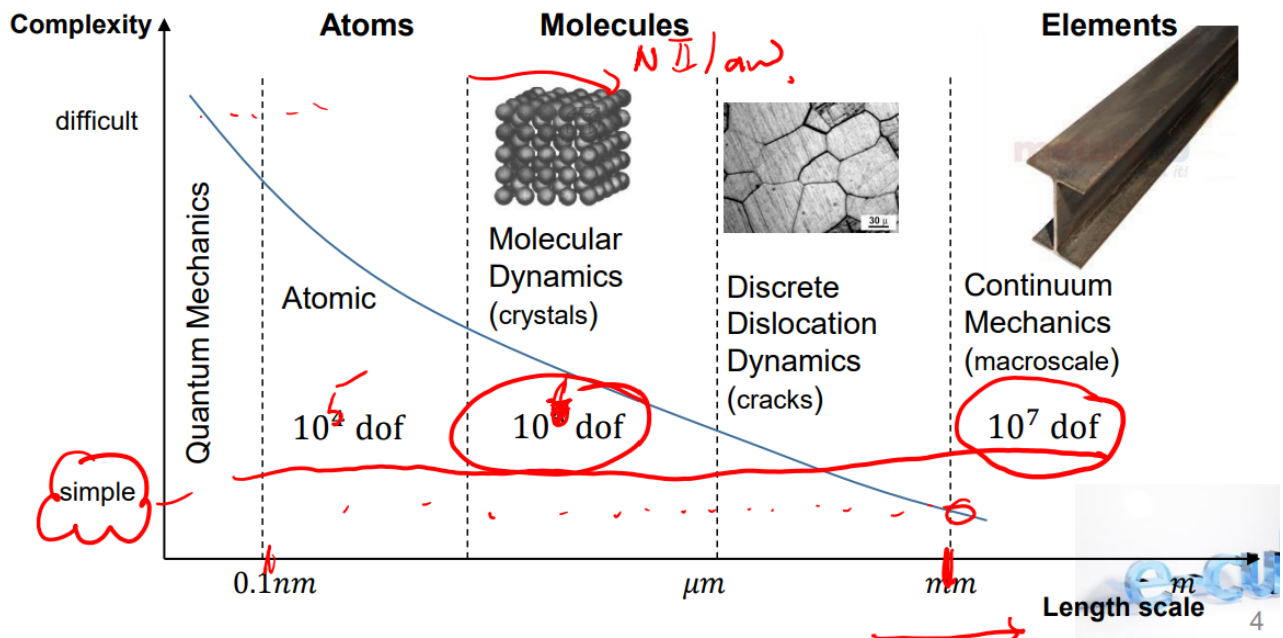


Figure 1.2: Graph to show complexity against scale.

1.1.2 Why focus on small scales?

- Small scale defects lead to crack initiation and propagation under external loading
- Failure can be corrected by changing material properties, for example, toughness
- Source of defects: complex chemical process (chemistry / corrosion) leads to corrosion at the surface
- Macroscale process is linked to microscale action
- Hypersonic flow - ionisation is non-continuum effect
- Analogy between defective liquids / solids

Note: turbulence is controlled by small vortices.

Micrograph

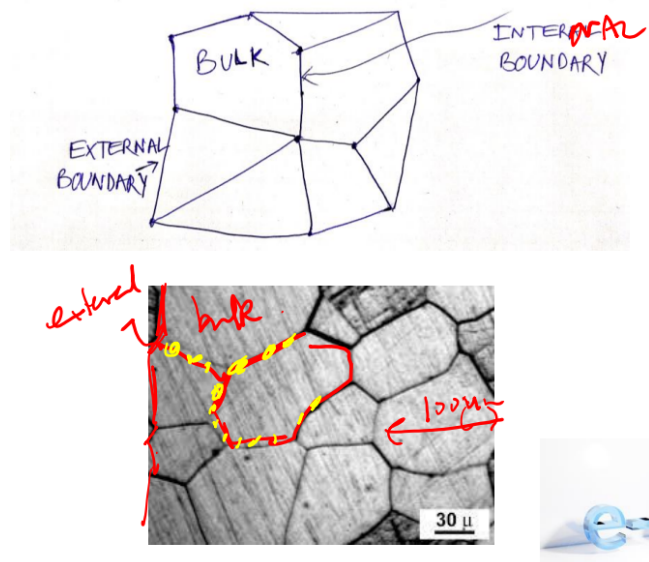


Figure 1.3: Graph to show complexity against scale.

Internal grain processes

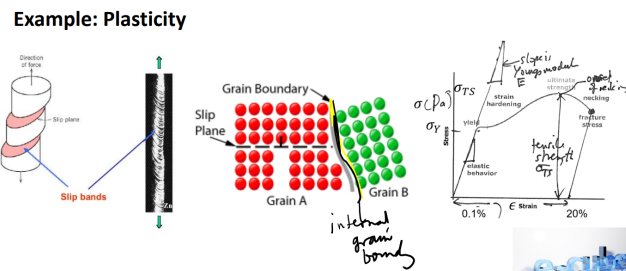


Figure 1.4: Example of plasticity from internal grain process level.

Internal boundary (hydrogen embrittlement - plastic deformation / slip)

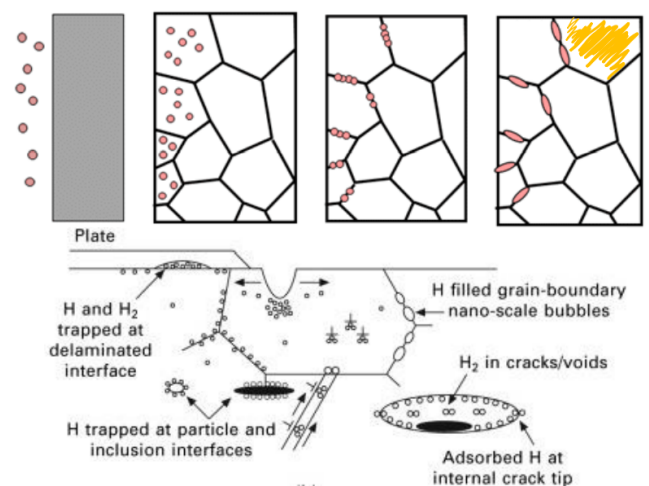


Figure 1.5: Hydrogen embrittlement - plastic deformation / slip

Matter	Modelling approach	
Solid	Atomistic	Continuum
Gas	Kinetic theory	Continuum
Liquid	Molecular	Continuum

Table 1.3: Categorisation of matter

External boundary (corrosion)

Corrosion happens over a long time and a range of scales. We need to understand how ions move around and interact with materials.

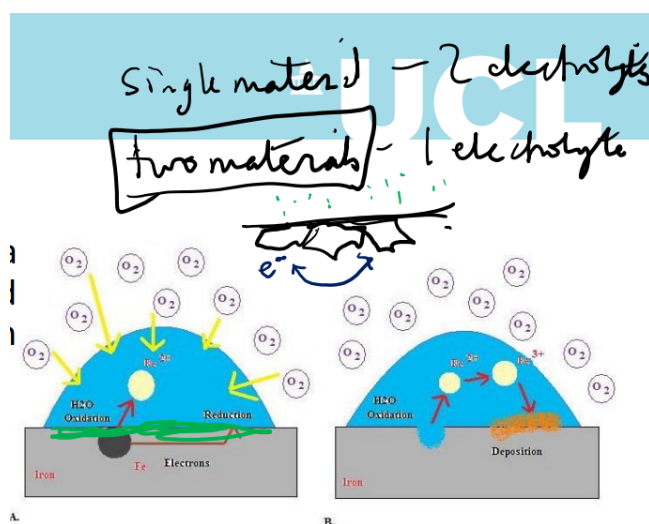
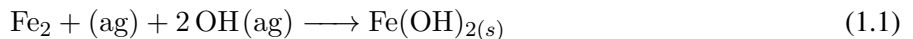


Figure 1.6: Rust corrosion from grain boundary level.

1.2 Categorisation of matter

Switch between states are due to p , V and T and is represented by phase diagram. States of matter have been part of most religious and scientific texts for the last two thousand years, with water (aqua), fire (ignis), air (aer) and earth (terra) with the fifth being the void.

1.3 Atomistic view of matter

Typical length scale:

- Diameter of atom is $0.1 \text{ nm} = 1 \times 10^{-10} \text{ m} = 1 \text{ angstrom}$
- Nucleus diameter is $1 \times 10^{-15} \text{ m}$ (hydrogen) to $15 \times 10^{-15} \text{ m}$ (uranium-238)

1.3.1 Bulk characteristic of materials

The aim is to understand the relationship between the macrostructure and the microstructure. Key measures are:

- Young's modulus $E = \frac{d\sigma}{d\varepsilon} \Big|_{\varepsilon \rightarrow 0}$

Properties		Definition
Elastic modulus	E (Pa)	Measure of material resistance to deformation.
Yield stress	σ_Y (Pa)	Measure of stress at which the elastic behaviour disappears and plastic behaviour initiates.
Hardness	HBW	Measure of material resistance to indentation
Creep		Time-dependant deformation at high temperature and constant stress.
Toughness	K (J m^{-3})	Resistance to crack propagation.
Ductility	ϵ_T	Material's ability to undergo plastic deformation.

Table 1.4: Key points on material properties

- Tensile stress: σ_{TS}
- Yields stress: σ_Y
- Ductility: ϵ_T

It is important to understand the following: How are they related to the microstructure?

1.3.2 Newtonian model of matter

Useful for biological, physical problems, solids, liquids and gases. This is based on a description of matter as a collection of point particles, an approach that is useful for gases, liquid and solids. The dynamics of the i-th molecule is:

$$\underline{F}_i = \sum_{j,j} \neq \nabla U(x_i, x_j) \quad (1.3)$$

Located at point \underline{x}_i whose dynamics are:

$$m_i \frac{d\underline{v}_i}{dt} = \underline{F}_i \quad (1.4)$$

$$\underline{v}_i = \frac{d\underline{x}_i}{dt} \quad (1.5)$$

The formulation requires the form of the interaction stated using the Lennard-Jones 6-12 potential:

$$U = 4\epsilon \left(\left(\frac{\sigma}{r} \right)^{12} - \left(\frac{\sigma}{r} \right)^6 \right) + \dots \quad (1.6)$$

The difficulty is that neighbourhood lists are kept and only sum over local interaction of molecules.

- Not hard collision
- Time stepping fixed
- Potentials can be empirical or chosen to now slow down calculations

$$U = U_{stretch} + U_{bend} + U_{torsion} + U_{vanderWaals} + U_{electro} + U_{cross} \quad (1.7)$$

Research gaps:

- Link between continuum and molecular
- Quantim - mechanical models

1.3.3 Vibrational modes and energy

Mechanical representation of matter. Molecules interact with their neighbours and fields. Interaction may be quite far, particularly when charges are important. We are familiar with how degrees of freedom influence properties of a gas, especially through the isentropic index. Energy is stored in various modes of vibration e.g. gas. This is called classical molecular dynamics.

1.3.4 Molecular description of material properties

Primary bonds

Ionic and covalent bonds are extremes with most (electron distribution) bonds lying between (polar covalent)

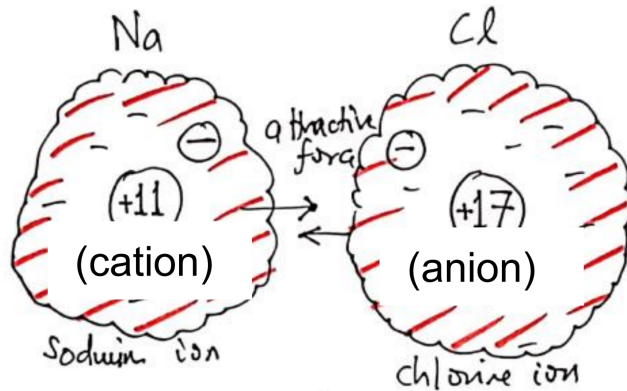


Figure 1.7: Ionic bond (electrovalence)

$$F = \frac{q_1 q_2}{4\pi\epsilon_0 r^2} \quad (1.8)$$

$$U = U_i - \frac{q^2}{4\pi\epsilon_0 r} + \frac{B}{r^n} \quad (1.9)$$

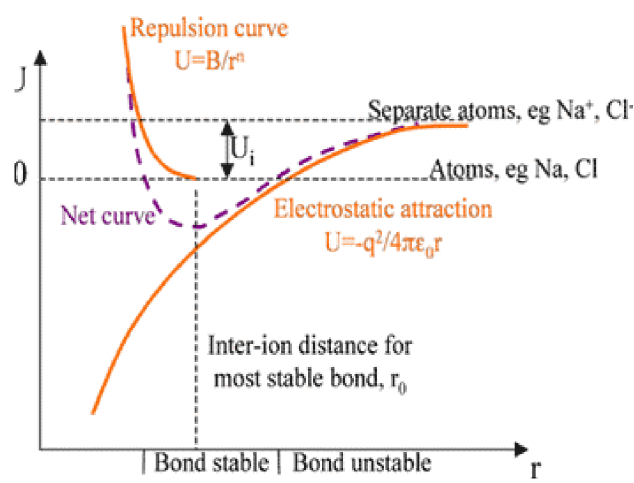


Figure 1.8: Bond stability.

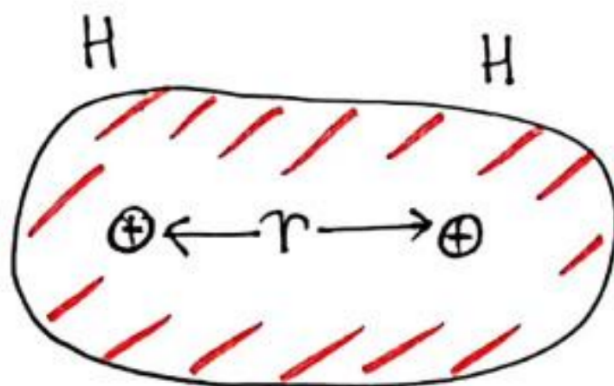


Figure 1.9: Covalent bond (covalence). Note the overlap of electron orbit.

$$U = -\frac{A}{r^m} + \frac{B}{r^n}, \quad m < n \quad (1.10)$$

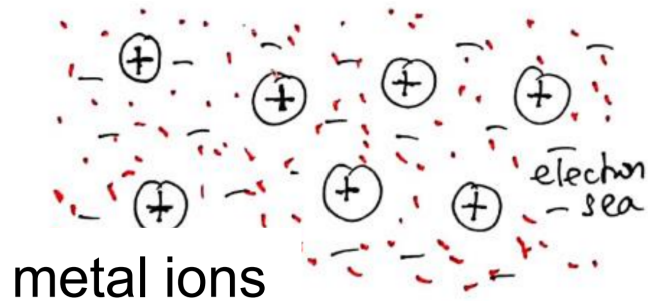


Figure 1.10: Metallic bond (electron cloud).

$$e = 1.6 \times 10^{-19} \text{ C} \quad (1.11)$$

$$\epsilon_0 = 8.8 \times 10^{-12} \text{ Nm}^2 \text{C}^{-2} \quad (1.12)$$

$$1 \text{ eV} = 1.6 \times 10^{-19} \text{ J} \quad (1.13)$$

Secondary bonds

The secondary bonds are important - without them many gases would not condense. The relative displacement of the positive and negative charge gives rise to a dipolar force. This gives rise to an attractive force. Most usual form is the Lenard Jones 6-12 potential.

$$U = -\frac{A}{r^6} + \frac{B}{r^n} \quad (1.14)$$

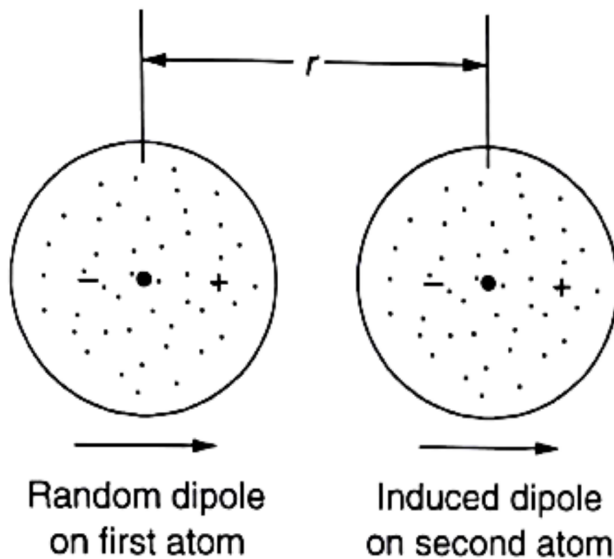


Figure 1.11: Secondary bonds. Note: long range attractive force - dipole-dipole interactions. Overlapping electron orbits - repulsive.

Physical basis of Young's Modulus

Classical mechanics:

$$m \frac{dv}{dt} = \frac{dU}{dr} \quad (1.15)$$

where U is the potential energy. At equilibrium:

$$\frac{dU}{dr} = 0 \quad (1.16)$$

so that close to this point, the energy potential can be expanded to give:

$$m \frac{d^2 r}{dt^2} = \left(\frac{d^2 U}{dr^2} \right) (r - r_0) \quad (1.17)$$

Around equilibrium point:

$$F = S_0 (r - r_0) \quad (1.18)$$

$$S_0 = - \frac{d^2 U}{dr^2} \quad (1.19)$$

The stress is:

$$\sigma = NS_0 (r - r_0) = \frac{S_0 (r - r_0)}{r_0^2} \quad (1.20)$$

The Young's modulus is:

$$E = \frac{\sigma}{\epsilon} = \frac{S_0}{r_0} \quad (1.21)$$

Estimate:

$$S_0 = \frac{\alpha q^2}{4\pi\epsilon_0 r^2} \quad (1.22)$$

$$E = \frac{\sigma}{\epsilon} = - \frac{\frac{d^2 U}{dr^2}}{r_0} = \frac{\delta e^2}{4\pi\epsilon_0 r_0^4} \quad (1.23)$$

Atom spacing:

$$\bar{r}_0 \approx 8.54$$

(1.24)

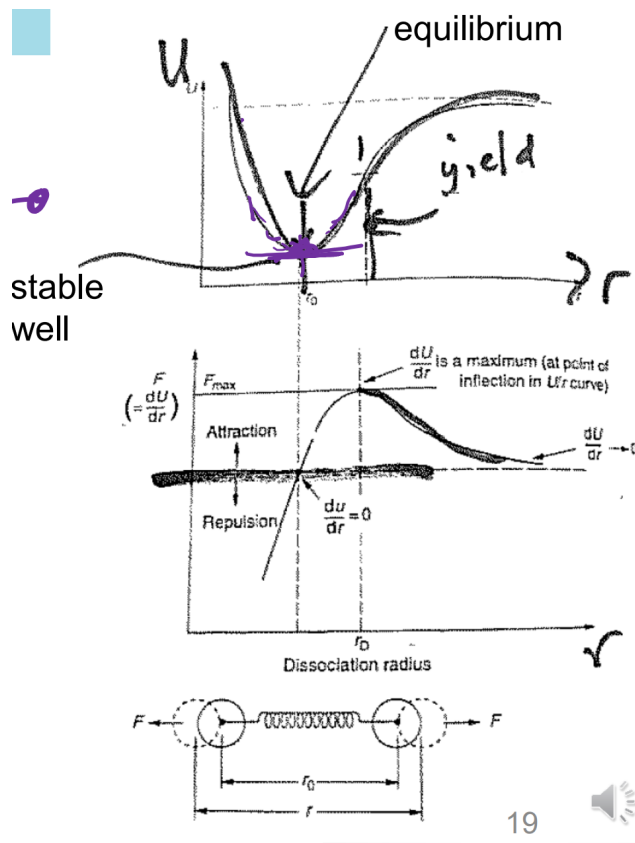


Figure 1.12: Young's modulus from atomic perspective.

Comparison between molecular and macroscopic measurements

Bond type	S_0 / Nm^{-1}	Young's modulus estimate E / GPa	Measurement
Covalent	50 - 180	200 - 1000	1000 (diamond)
Metallic	15 - 75	60 - 300	200 (nickel)
Ionic	8 - 24	32 - 96	15 - 91 (alkali halides)
H-Bond	2 - 3	8 - 12	9.1 (ice)
van der Waals	0.5 - 1	2 - 4	0.01 - 2 (rubber to nylon)

Table 1.5: Comparison between molecular and macroscopic measurements.

Estimation of yield stress

Returning to the molecular model since:

$$U = \epsilon \left(-\frac{A}{r^6} + \frac{B}{r^{12}} \right) \quad (1.25)$$

$$U'' = \epsilon \left(-\frac{6 \times 7A}{r^8} + \frac{12 \times 13B}{r^{14}} \right) \quad (1.26)$$

Then, maximum stress is:

$$\sigma_Y \approx \frac{E}{8} \quad (1.27)$$

Therefore:

$$\frac{\sigma_Y}{E} \frac{1}{8} \quad (1.28)$$

This estimated ratio is good for ceramics, but not good for metals. So what is missing from a molecular description?

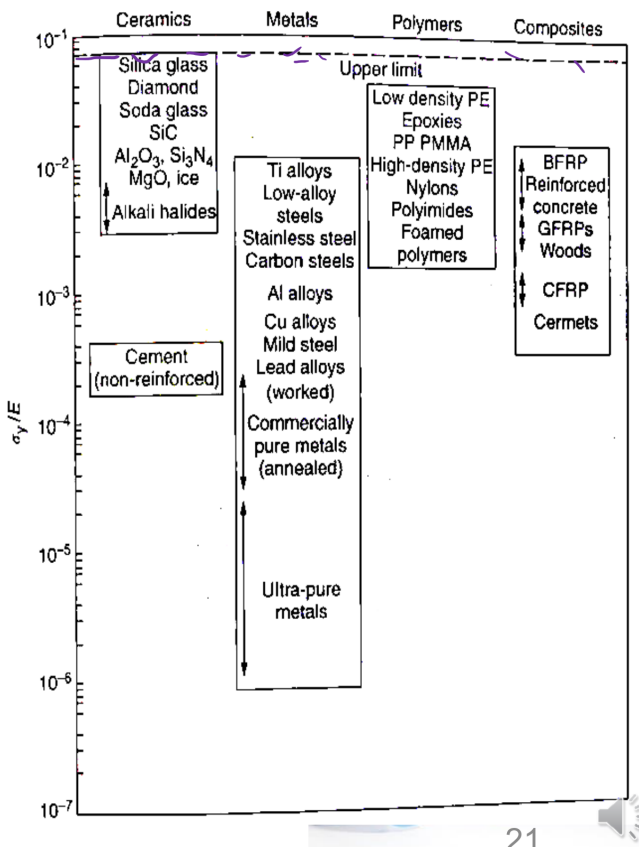


Figure 1.13: Graph to show yield stress ratio for different materials.

1.3.5 Material classification

- Metals
 - Ferrous metals and alloys
 - Non ferrous metals and alloys
 - (focus on here)
- Polymeric (non metallic, non crystalline)
 - Thermoplastic plastics
 - Thermoset plastics
 - Elastomers
- Ceramics
 - Glass
 - Diamond
 - Glass ceramics
- Composites (everything else)

- Metal-matrix composites
- Sandwich structures
- Concrete

Three common configurations

Type	Name	Description	Example
BCC	Body centred cube - 2 atoms	Harder and less malleable Packing factor 0.68	Lithium, Sodium, Potassium
FCC	Face centred cube	malleable, softer 0.74	Chromium, Barium, Alpha-iron Copper, Gold, Aluminium Iridium, Lead, Nickel, etc.
HCP	Hexagonal close packed	6 atoms Packing ratio 0.74	Cadmium, Magnesium, Titanium Zinc, Zirconium

Table 1.6: Configurations of atoms.

Solidification and crystal growth

Under normal circumstances, crystal growth starts at many nucleation points. Solidification leads to crystals growing and stop growing when they meet another crystal. A crystal is usually called a grain. The boundary between grains is the grain boundary where structure is disordered. This is controlled using nucleation points and directional solidification and liquid freezing-dendritic growth and shrinkage occurs during cooling.

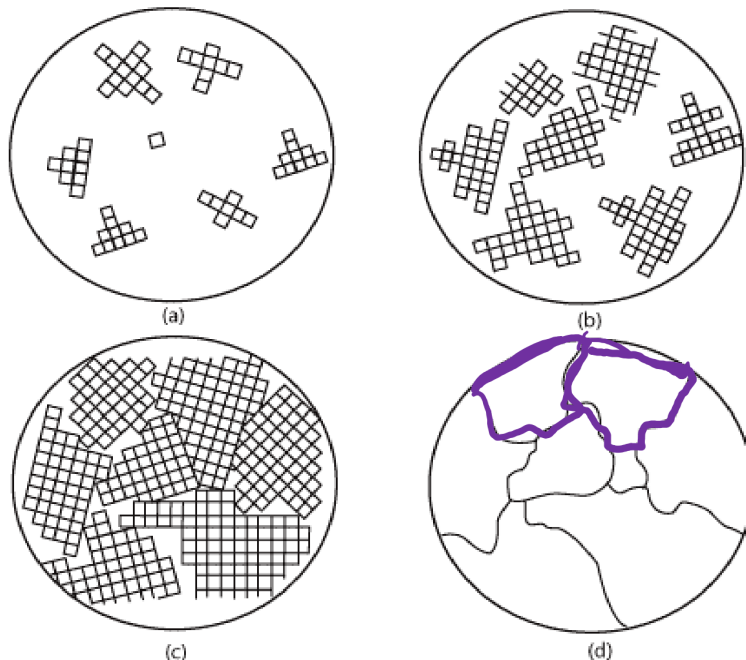


Figure 1.14: Nucleation of crystals.

Crystal defects

Three types of defects:

1. Point defects: which are places where an atom is missing or irregularly placed in the lattice structure.
Point defects include lattice vacancies, self interstitial atoms, substitution impurity atoms and interstitial impurity atoms

2. Linear defects: which are groups of atoms in irregular positions. Linear defects are commonly called dislocations
3. Planar defects: which are interfaces between homogeneous regions of the material. Planar defects include grain boundaries, stacking faults and external surfaces

Atomistic view of plastic deformation

Elastic deformation - stress is small, the metal can recover to initial state when the stress is removed. This involves stretching the bonds but atoms do not move over one another.

Plastic deformation - stress is large, plastic deformation involves the breaking of a limited number of atomic bonds by the movement of dislocations. Since the energy required to move is lowest along the densest planes of atoms, dislocations have a preferred direction of travel within a grain of the material. This results in slip that occurs along parallel planes within the grain. These parallel slip planes group together to form slip bands. A slip band appears as a single line under the microscope, but it is in fact made up of closely spaced parallel slip planes as shown in the image.

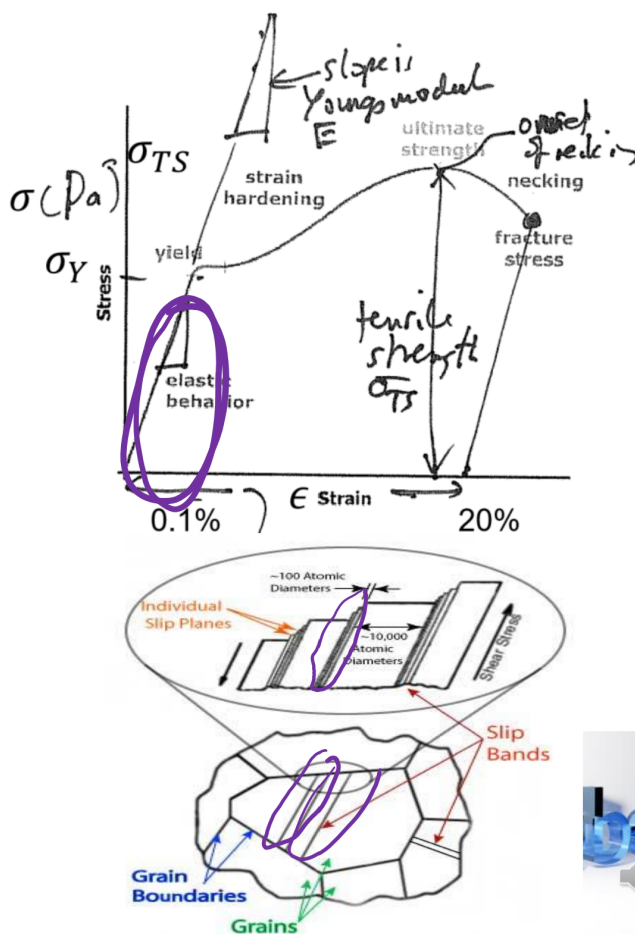


Figure 1.15: Stress-strain curve.

Fatigue crack initiation

The life of a fatigue crack has two parts, initiation and propagation. Dislocations play a major role in the fatigue crack initiation phase. It has been observed in laboratory testing that after a large number of loading cycles dislocation pile up and form structures called persistent slip bands. Initiation has a molecular origin.

Topological change in crystal structure

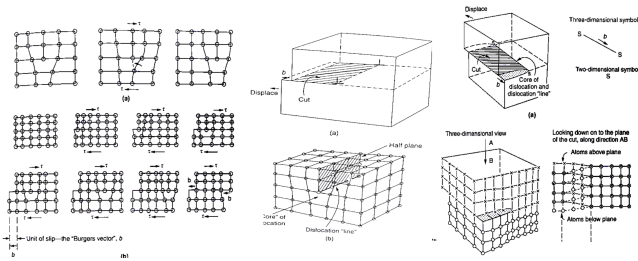


Figure 1.16: Topological changes in crystal structure.

1.4 Kinetic theory of gases

Statistical 19th century view of macroscopic properties of gas. Boltzmann and colleagues developed new techniques to describe matter. Heavily influenced the theory of turbulence ← based on kinetic theory of a gas.

$p = \rho RT$ origin with statistical theory.

This is an excellent macroscopic model of matter. The problem is that it does not work well for low pressure, high pressure or when density is low (and continuum concepts don't work).

1.4.1 Speed of molecules

Results tell us about average speed but not the distribution.

$$n_v(E) = n_0 e^{-\frac{E}{k_B T}} \quad (1.29)$$

where, $n_v(E)$ is the Boltzmann distribution which coups a lot. The speed of the molecules satisfies the Maxwell-Boltzmann distribution.

$$f(v) = 4\pi \left(\frac{m}{2\pi k_B T} \right)^{\frac{3}{2}} v^2 \exp \left(-\frac{mv^2}{2k_B T} \right) \quad (1.30)$$

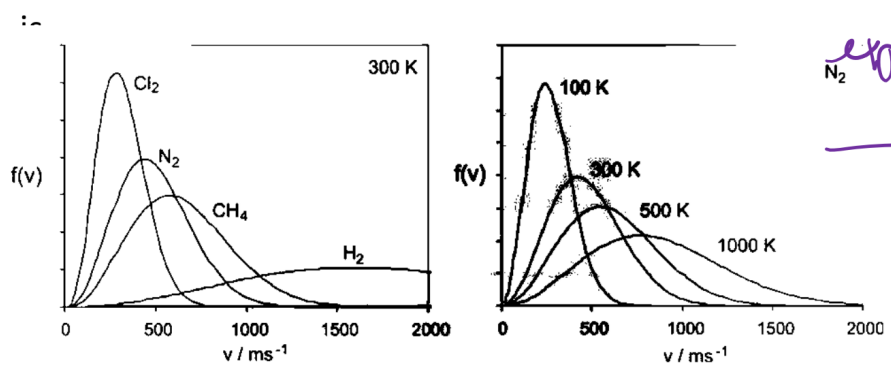


Figure 1.17: Speed of molecules.

1.4.2 Equations of state of real gases

The molecular continuum view of matter are linked. Virial equation:

$$pV = nRT \left(1 + \frac{B}{V_m} + \frac{C}{V_m^2} + \dots \right) \quad (1.31)$$

where B, C are the second and third virial coefficients. Van der Waals equation:

$$\left(p + a \frac{n^2}{V^2} \right) (V - nb) = nRT \text{ or} \quad (1.32)$$

$$P = \frac{nRT}{V - nb} - a \frac{n^2}{V^2} \quad (1.33)$$

n is the number of moles. nb is the volume excluded since molecules cannot overlap. $\frac{an^2}{V^2}$ pressure reduced due to attractions between pairs of molecules.

Critical constants for van der Waals equation

Solving these two equations in two unknowns (temperature and molar volume) gives the critical temperature and critical molar volume:

$$T_c = \frac{8a}{27Rb} \quad (1.34)$$

$$V_c = 3b \quad (1.35)$$

Van der Waals

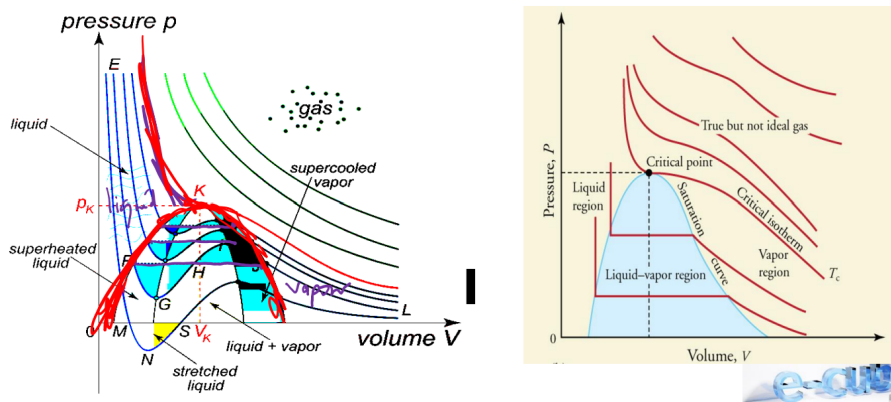


Figure 1.18: Van der Waals.

Link between molecular and microscopic

Most of the important 19th century breakthroughs were determining link between macroscopic (could be seen) and microscopic (could not be seen). For example, Brownian motion:

$$\frac{RT}{5\pi\mu dN_A} = D = \lim_{t \rightarrow \infty} \frac{(x^2)}{2t} \approx 10 \times 10^{-10} \text{ m}^2 \text{ s}^{-1} \quad (1.36)$$

This represented a link between Avogadro's constant and macroscopic movement of particles. Here $N_A = 6 \times 10^{23} \text{ mol}^{-1}$. Theory by Einstein (1905) and Sutherland (1905). Millikan's experiments: determination of the charge on an electron. The link between molecular and microscopic last areas of modern science to be worked out.

Einstein theory and Millikan's experiment

Based around kinetic theory of gases and momentum change due to collision. Pressure is a manifestation of a:

$$P = \frac{2}{3} \frac{N}{V} \frac{1}{2} m_0 \bar{v}^2 \quad (1.37)$$

$$\therefore PV = nRT = \frac{N}{N_a} RT = Nk_B T \quad (1.38)$$

$$\therefore KE = \frac{3}{2} N k_B T = \frac{3}{2} nRT = \frac{NDF}{2} nRT \quad (1.39)$$

where NDF is number of degrees of freedom.

Model assumptions

- No intermolecular forces between the gas particles
- The volume occupied by the particles is negligible compared to the volume of the container they occupy
- The only interactions between the particles and with the container walls are perfectly elastic collisions.
- Real gas, the atoms or molecules have a finite size, and at close range they interact with each other through a variety of intermolecular forces, including dipole-dipole interactions, dipole induced dipole interactions and van der Waal's (induced dipole - induced dipole) interactions
- When applied to real gases, the ideal gas model breaks down when molecular size effects or intermolecular forces become important. This occurs under conditions of high pressure, when the molecules are forced close together and therefore interact strongly, and at low temperatures, when the molecules are moving slowly and intermolecular forces have a long time to act during a collision

The pressure at which the ideal gas model starts to break down will depend on the nature and strength of the intermolecular forces between the gas particles, and therefore on their identity. The ideal gas model becomes more and more exact as the pressure is lowered, since at very low pressures the gas particles are widely spaced apart and interact very little with each other.

$$\text{number density} = \frac{N}{V} = \frac{nN_A}{V} \quad (1.40)$$

$$\Delta p_x = (2mv_x) \left(\frac{1}{2} \frac{nN_A}{V} Av_x \Delta t \right) = \frac{nMAv_x^2 \Delta t}{V} \quad (1.41)$$

$$p = \frac{F_x}{A} = \frac{nMv_x^2}{V} \quad (1.42)$$

1.5 Chemistry for engineers

Chemistry has a molecular origin. The engineering challenge is how to include chemistry into multiphysics problems. Chemistry might be simple:



Part II

Extreme Temperature

Chapter 2

How to Cool Very Hot Surfaces

2.1 Introduction

Context	Material development	Design
Gas turbine engines	Material development manufacturing techniques	TBC air cooling
Re-entry spacecraft	Surface properties ablation	Angle of attack changing geometry
Silicon processors	None really - still with silicon with an adhesive metal plate	Clamp on cooling system

Table 2.1: Introduction.

2.2 Jet engines

Purpose is to convert chemical energy into linear momentum (IC engine - chemical energy into pressure).

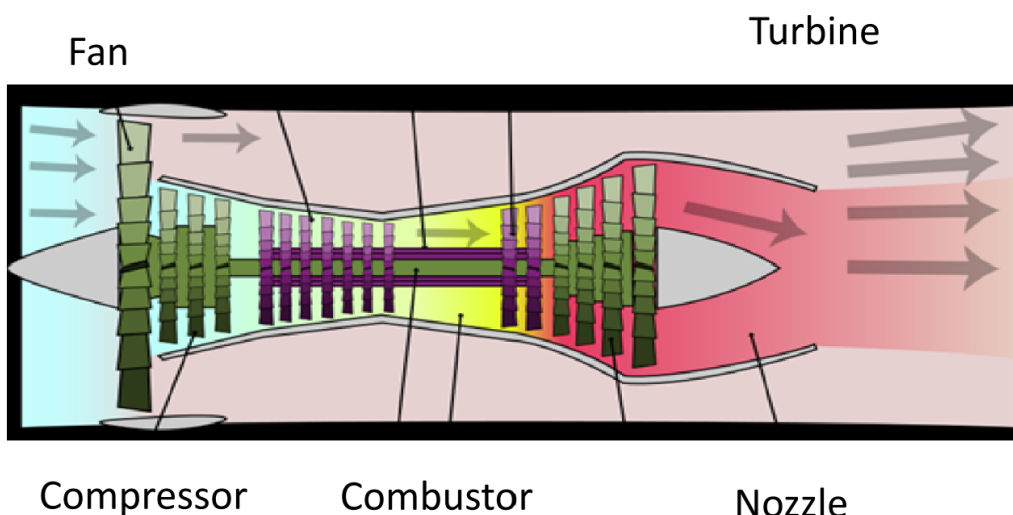


Figure 2.1: Jet engine.

2.2.1 Brayton (or Joule) cycle

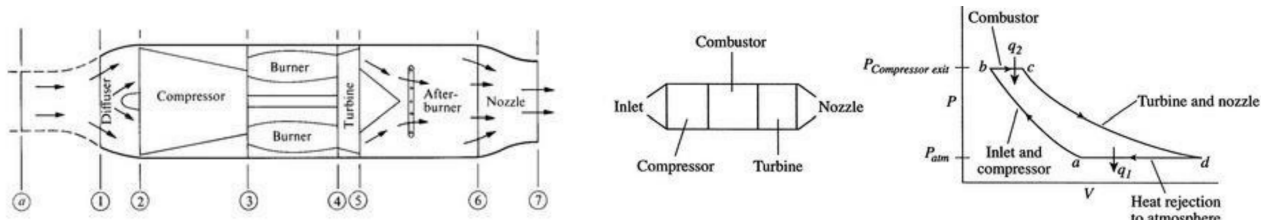


Figure 2.2: Brayton (or Joule) cycle.

- a-b: adiabatic, quasi-static (or reversible) compression in the inlet and compressor
- b-c: constant pressure fuel combustion (idealised as constant pressure heat addition)
- c-d: adiabatic, quasi-static (or reversible) expansion in the turbine and exhaust nozzle, with which we take some work out of the air and use it to drive the compressor and take the remaining work out and use it to accelerate fluid for jet propulsion, or to turn a generator for electrical power generation
- d-a: cool the air at constant pressure back to its initial condition
- **Fan** - the large spinning fan sucks in large quantities of air. It then speeds this air up and splits it into two parts. One part continues through the “core” or centre of the engine, where it is acted upon by the other engine components. The second part “bypasses” the core of the engine. It goes through a duct that surrounds the core to the back of the engine where it produces much of the force that propels the airplane forward. The cooler air helps to quiet the engine as well as adding thrust to the engine.
- **Compressor** - the compressor is the first component in the engine core. The compressor squeezes the air that enters it into progressively smaller areas, resulting in an increase in the air pressure. This results in an increase in the energy potential of the air. The squashed air is forced into the combustion chamber.
- **Combustor** - in the combustor the air is mixed with fuel and then ignited. This provides a high temperature, high-energy airflow. The fuel burns with the oxygen in the compressed air, producing hot expanding gases. The inside of the combustor is often made of ceramic materials to provide a heat-resistant chamber. The temperature can reach 2700 °C
- **Turbine** - the high-energy airflow coming out of the combustor goes into the turbine, causing the turbine blades to rotate. The turbines are linked by a shaft to turn the blades in the compressor and spin the intake fan at the front. This rotation takes some energy from the high-energy flow that is used to drive the fan and the compressor. The gases produced in the combustion chamber move through the turbine and spin its blades. The turbines of the jet spin around thousands of times. They are on fixed shafts which have several sets of ball-bearings in between them.
- **Nozzle** - the nozzle produces the thrust for the plane. The energy depleted airflow that passed the turbine in addition to the colder air that bypassed the engine core, produces a force when exiting the nozzle that acts to propel the engine, and therefore the airplane, forward. The combination of the hot air and cold air are expelled and produce an exhaust, which causes a forward thrust. The nozzle may be preceded by a mixer, which combine the high temperature air coming from the engine core with the lower temperature air that was bypassed in the fan. The mixer helps to make the engine quieter.

2.2.2 Typical values

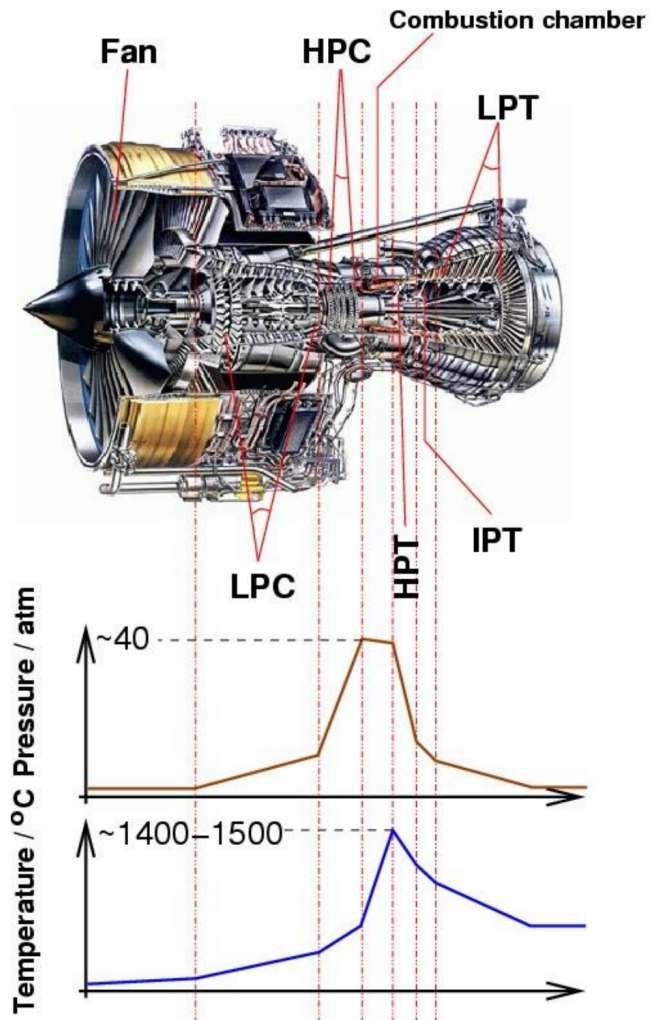


Figure 2.3: Typical temperature values for different stages of cycle in bypass gas-turbine engine.

Metal	Melting point
Titanium	1668 °C
Nickel	1455 °C
Steel	1370 °C

Table 2.2: Table to show melting points of various metals used in bypass gas-turbine engines.

Combustion at about 1800-1900 °C. Large centrifugal acceleration 25 000 rpm for large engines 500 000 rpm for micro gas turbine. Higher temperature makes the thermodynamic efficiency greater (about 60%). Combustion temperature is above melting point of metals.

Fuel	Combustion temperature
Methane (in air)	1950 °C
Hydrogen (in air)	2110 °C
Propane (in oxygen)	2880 °C

Table 2.3: Table to show combustion temperatures of various fuels.

Meeting the needs

1. Choice of material
2. Manufacturing technique
3. Design

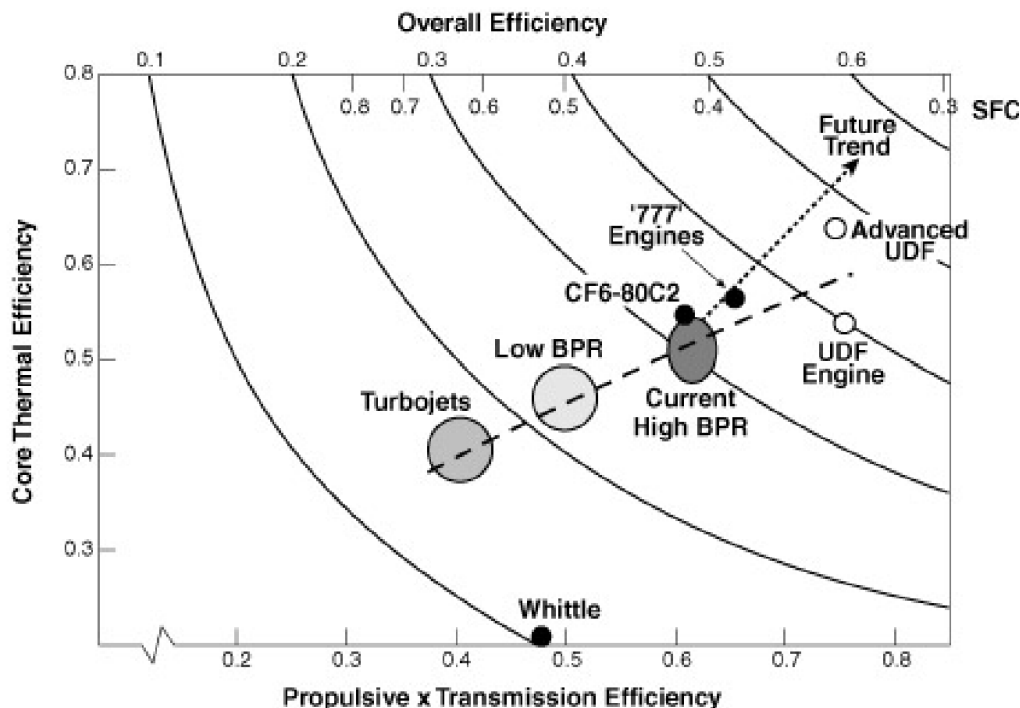


Figure 2.4: Efficiencies of various gas-turbine engines.

2.2.3 Material selection

Considerations:

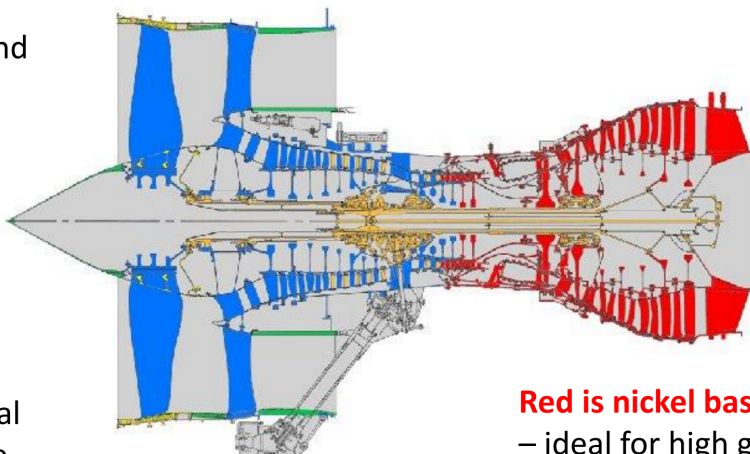
1. Strength and weight: titanium
2. Temperature: major constraint is the material selection for the hot section (combustor and turbine) of the engine

The need for better materials spurred much research in the field of alloys and manufacturing techniques, and that research resulting in a long list of new materials and methods that make modern gas turbines possible. One of the earliest of these was Nimonic 90 (nickel-based, high-temperature, low-creep superalloys Ni 54%, Cr 18-21%, Co 15-21%, Ti 2-3%, Al 1-2%).

The development of superalloys in the 1940s and new processing methods such as vacuum induction melting in the 1950s greatly increased the temperature capability of turbine blades. Further processing methods like hot isostatic pressing improved the alloys used for turbine blades and increased turbine blade performance. Modern turbine blades often use nickel-based superalloys that incorporate chromium, cobalt and rhenium.

Blue is titanium –

ideal for strength and density and low temperatures



Orange – steel – ideal for static parts of the compressor high temperature.

Red is nickel based superalloys

- ideal for high gas temperature
- entrance temperature is 1400°C , cooling system (surface temp 1100°C) with coating is 930°C

Figure 2.5: Usage of different alloys within the engine.

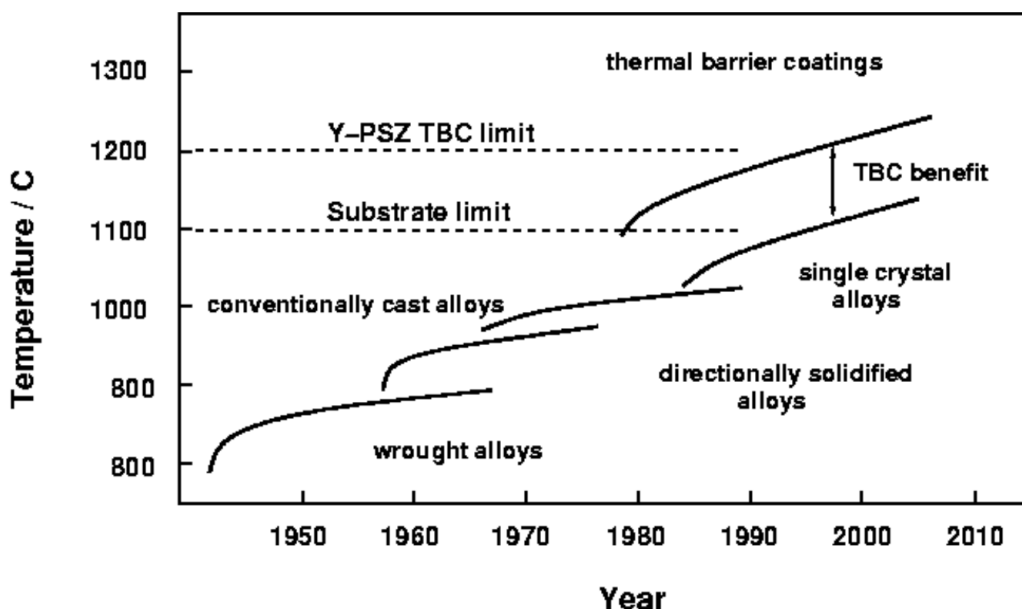


Figure 2.6: Development of alloys.

Titanium - good for weight and strength (poor with heat).

Alloy improvement, directional and single-crystal solidification have contributed significantly, but arguably, the emphasis has been shifted to coating systems which have allowed an increase of gas temperatures up to 1100°C . Coatings in gas turbines serve a variety of purposes. A first requirement to operate turbines at higher temperatures was, of course, improved strength. Unfortunately, these conditions also mean severe oxidation / corrosion problems, and to make things worse, the improvement in mechanical properties of the base alloys was made at the expense of environmental resistance.

The first purpose of coatings was to improve poor oxidation resistance of the base alloy (aluminide, Pt-aluminide, MCrAlY). A second type of coatings applied to high-temperature parts are known as thermal barrier coatings (TBC). These are ceramic coatings with very low thermal conductivity and thin ($200\ \mu\text{m}$). Drop of $100\text{-}300^{\circ}\text{C}$ between the gas and metal surface temperatures but are ‘oxygen transparent’ and do not prevent

oxidation of the underlying substrate.

2.2.4 Manufacturing process

Aside from the alloy improvements, a major breakthrough was the development of directional solidification (DS) and single crystal (SC) production methods. These methods help greatly increase strength against fatigue and creep by aligning grain boundaries in one direction (DS) or by eliminating grain boundaries altogether (SC).

Recent generations of superalloys for single crystal turbine blades contain relatively high percentages of refractory elements such as Ta, W or Re which enhance the high-temperature mechanical properties.

This is done at the expense of Cr and Al. Given the severe environmental conditions in which the blades operate, the removal of the elements (beneficial for oxidation resistance) implies even greater degradation problems.

To reduce the oxidation corrosion resistance, an external coating is applied to the blades. Its purpose is to allow for the growth of a resistant oxide layer. Of all possible oxides $\alpha\text{-Al}_2\text{O}_3$ offers excellent protection and very low growth rates (in a minority of cases, Cr oxides are preferred). The composition of the coating must therefore be chosen carefully so as to ensure growth of $\alpha\text{-Al}_2\text{O}_3$.

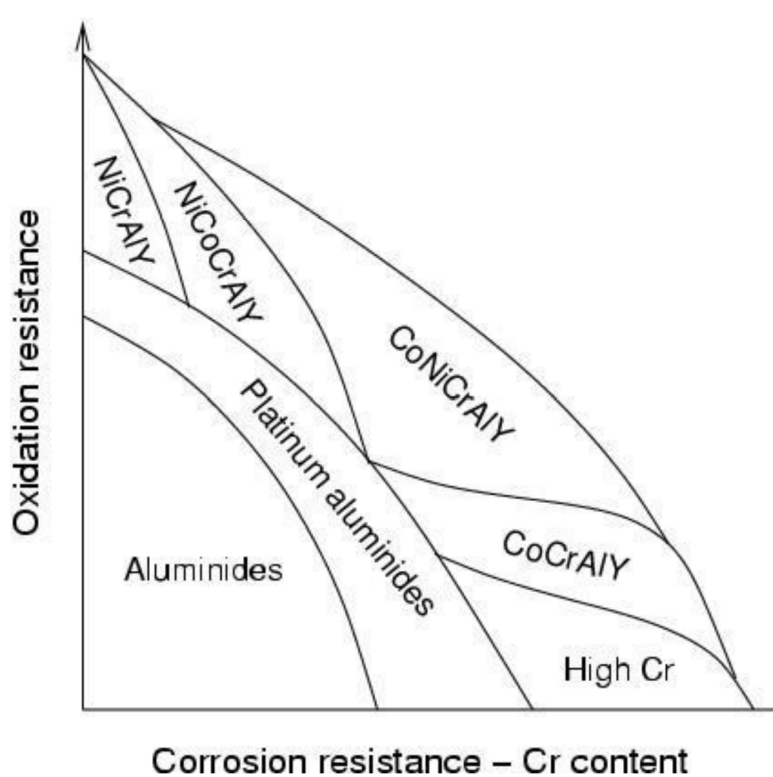


Figure 2.7: Oxidation and corrosion resistance of different alloys.

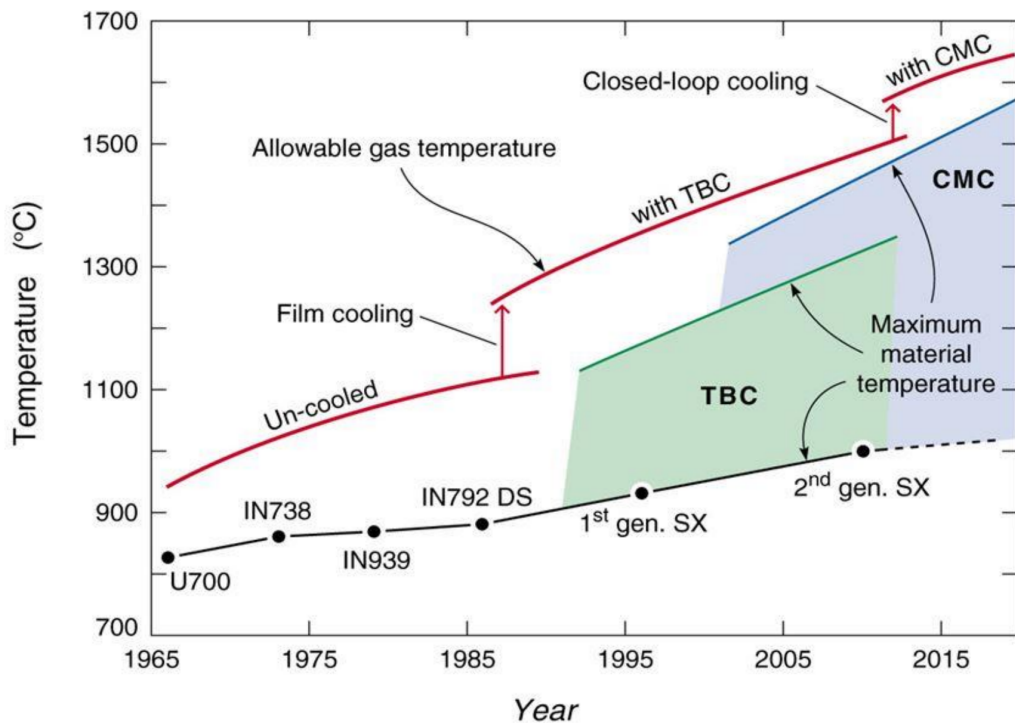


Figure 2.8: Temperature resistance of TBCs and CMCs over the years.

TBC - thermal barrier coating. CMC - ceramic matrix composite.

2.2.5 Thermal barrier coating

Thermal barrier coatings (TBC) are advanced materials systems usually applied to metallic surfaces, such as on gas turbine or aero-engine parts, operating at elevated temperatures, as a form of exhaust heat management. These 100 µm to 2 mm coatings serve to insulate components from large and prolonged heat loads by utilising thermally insulating materials which can sustain an appreciable temperature difference between the load-bearing alloys and the coating surface.

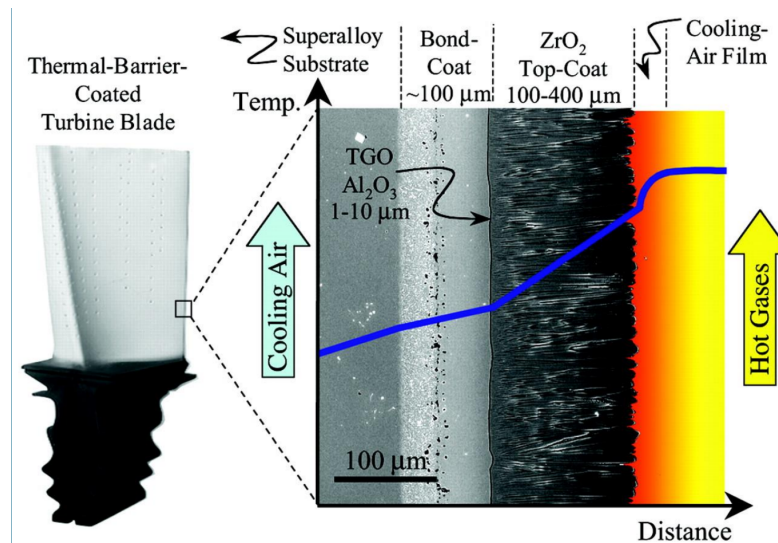


Figure 2.9: Thermal barrier coatings (TBCs).

Four layers:

1. The metal substrate

2. Metallic bond coat
3. Thermally-grown oxide (TGO)
4. Ceramic topcoat. The ceramic topcoat is typically composed of yttria-stabilised zirconia (YSZ) which is desirable for having very low of conductivity while remaining stable at nominal operating temperatures typically seen in applications. This ceramic layer creates the largest thermal gradient of the TBC and keeps the lower layers at a lower temperature than the surface.

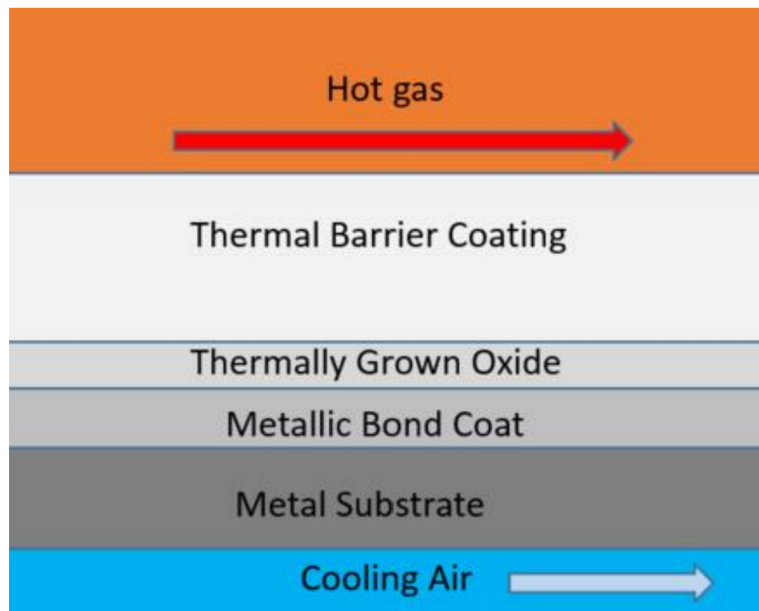


Figure 2.10: Thermal barrier coating composition.

TBCs improved corrosion and oxidation resistance, both of which became greater concerns as temperatures increased. First TBCs (1970s) were aluminide coatings. Ceramic coatings in 1980s which decreased turbine blade temperature by about 90 °C, improve blade life, almost doubling the life of turbine blades in some cases.

An effective TBC needs to meet certain requirements to perform well in aggressive thermo-mechanical environments. To deal with thermal expansion stresses during heating and cooling, adequate porosity is needed, as well as appropriate matching of thermal expansion coefficients with the metal surface that the TBC is coating.

1. A high melting point
2. No phase transformation between room temperature and operating temperature
3. Low thermal conductivity
4. Chemical inertness
5. Similar thermal expansion match with the metallic substrate
6. Good adherence to the substrate
7. Low sintering rate for a porous microstructure

These requirements severely limit the number of materials that can be used, with ceramic materials usually being able to satisfy the required properties.

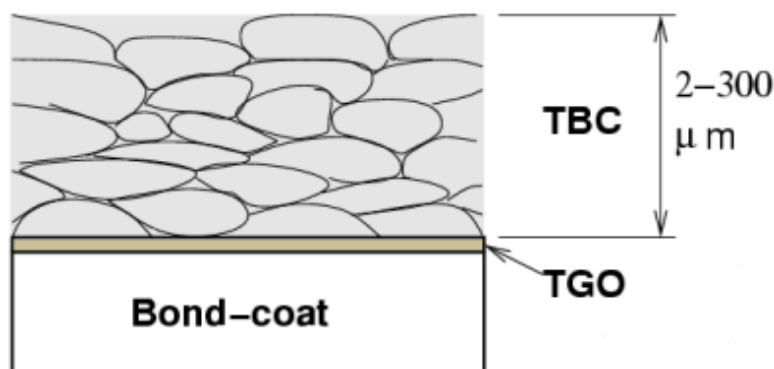


Figure 2.11: Microstructure of TBC.

For a ceramic coating to have any chance not to spall at the first thermal cycle, it is critical that its thermal expansion be close to that of the substrate. For the coating to be of use, it must also exhibit a very low thermal conductivity.

Thermal barrier coatings typically consist of four layers: the metal substrate, metallic bond coat, thermally-grown oxide (TGO), and ceramic topcoat. The ceramic topcoat is typically composed of yttria-stabilised zirconia (YSZ) which is desirable for having very low thermal conductivity while remaining stable at nominal operating temperatures typically seen in applications. This ceramic layer creates the largest thermal gradient of the TBC and keeps the lower layers at a lower temperature than the surface.

Most turbine blades are manufactured by investment casting (or lost-wax processing). This process involves making a precise negative die of the blade shape that is filled with wax to form the blade shape. If the blade is hollow (i.e. it has internal cooling passages), a ceramic core in the shape of the passage is inserted into the middle. The wax blade is coated with a heat-resistant material to make it a shell, and then that shell is filled with the blade alloy. This step can be more complicated for DS or SC materials, but the process is similar. If there is a ceramic core in the middle of the blade, it is dissolved in a solution that leaves the blade hollow. The blades are coated with a TBC, and then any cooling holes are machined. Ceramic matrix composites (CMC), where fibres are embedded in a ceramic matrix, are being developed for use in turbine blades. Main advantage of CMCs over conventional superalloys is their light weight and high temperature capability. SiC/SiC composites consisting of silicon matrix reinforced by silicon carbide fibres have been shown to withstand operating temperatures 100-200 °C higher than nickel superalloys.

Coating failure

TBCs fail through various degradation modes that include mechanical rumpling of bond coat during thermal cyclic exposure, especially coatings in aircraft engines; accelerated oxidation, hot corrosion, molten deposit degradation. There are also issues with oxidation (areas of the TBC getting stripped off) of the TBC, which reduces the life of the metal drastically, which leads to thermal fatigue.

A key feature of all TBC components is well matched thermal expansion coefficients between all layers. TBCs expand and contract at different rates upon heating and cooling of the environment, so when the different layers have poorly thermal expansion coefficients, a strain is introduced in the material which can lead to cracking and ultimately failure of the coating.

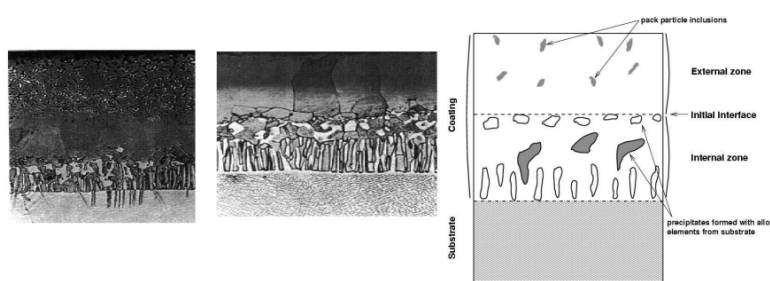


Figure 2.12: Failure of TBCs.

2.2.6 Corrosion processes

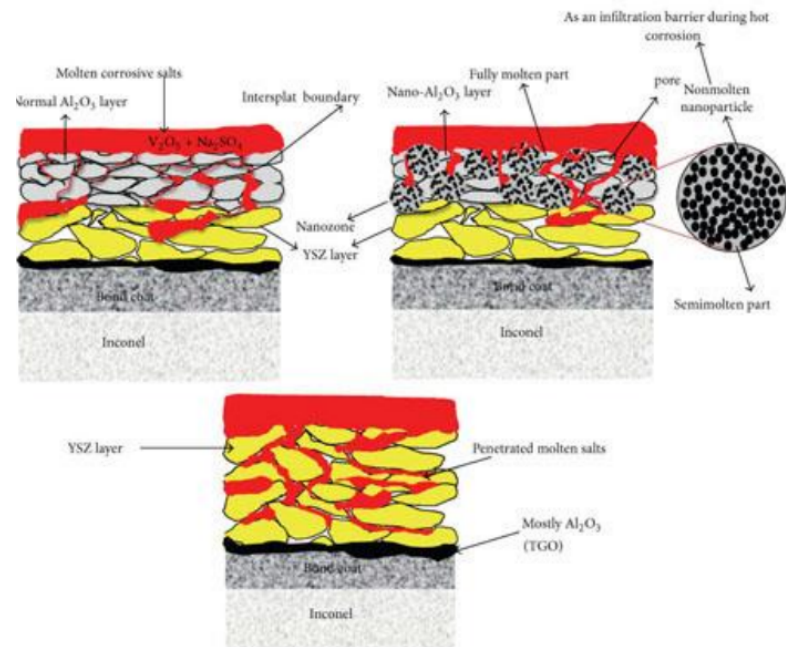


Figure 2.13: Schematic illustration of corrosive molten salts infiltration into the YSZ layer of different TBC coatings.

The high-pressure turbine of a jet turbine provides one of the most severe environments faced by man-made materials. To temperatures approaching the substrate melting point, one must add the considerable stresses caused by rotation at more than 10 000 rpm. Thermal barrier coating failure results in melting of the blade. Without reaching such catastrophic failure, blades suffer from accelerated oxidation or hot corrosion. Coatings can considerably enhance the oxidation/hot corrosion resistance of these components. Oxidation is the reaction between the coating (or in its absence, base alloy) with the oxidants present in the hot gases. Hot corrosion occurs from surface reactions with salts deposited from the vapour phase. This is caused by diffusion through the substrate alloy, as they are not in thermodynamic equilibrium with the latter.

2.2.7 Cooling through design

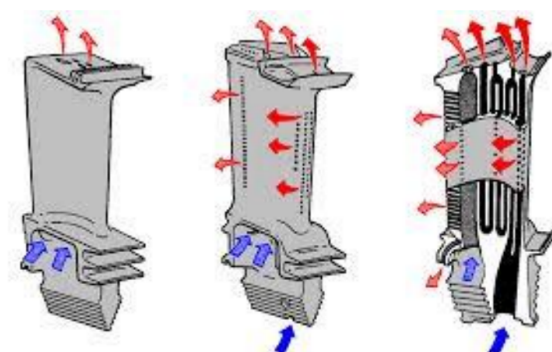
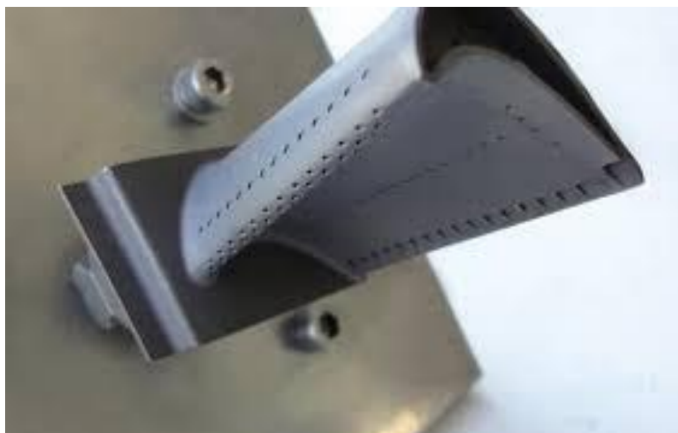


Figure 2.14: Cooling holes.



Figure 2.15: Blade with cooling holes.

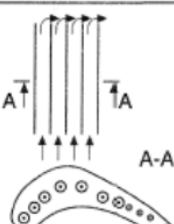
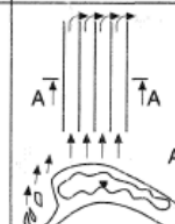
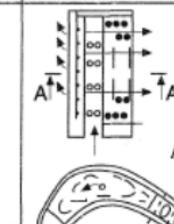
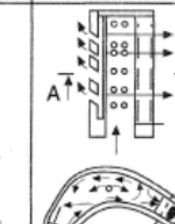
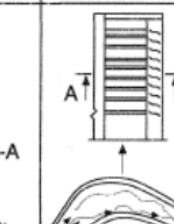
Main Data	Engine Type				
	JT8D-11(15)	JT9D-3A	JT9D-7	JT9D-59/70D	F-100
Tg, K	1294~1340	1420	1500	1598...1643	1590...1672
δ, %	~1,0	1,96	2.1	3.4	-3.0
θ	-0.2	-0.3	-0.45	-0.5	-0.55
Cooling system development	 Radial air flow ducts Multiflow - line schematic diagram of air flow	 Radial air flow ducts	 Deflector blade with air jet stream	 Film cooling and cooling air twisting 1.3% 1 + 2	 1. Deflector blade welded from two parts 2. Cooling air twisting 3. Development surface of inner finning

Table 2.4: Internal blade configurations.

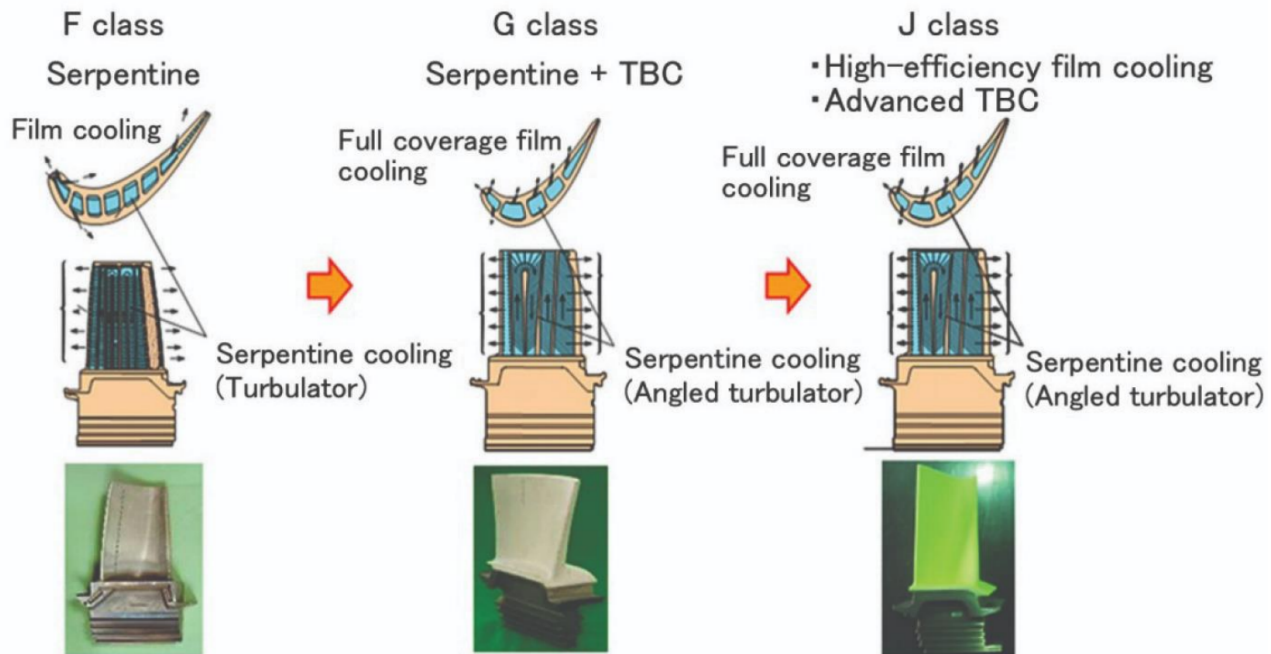


Figure 2.16: Classes of cooling technologies for internal blade cooling.

2.3 Atmospheric re-entry objects

Two types of entry:

1. Uncontrolled
2. Controlled (or EDL entry, descent and landing)

The kinetic energy of re-entry vehicles is enormous (50-1800 GJ) and thus must be expended. This is because this is the potential energy that must be lost. It is not possible to use retro rockets over whole descent as this uses too much fuel. Most objects require slowing down (except for ballistic warheads).

2.3.1 Idealised re-entry path

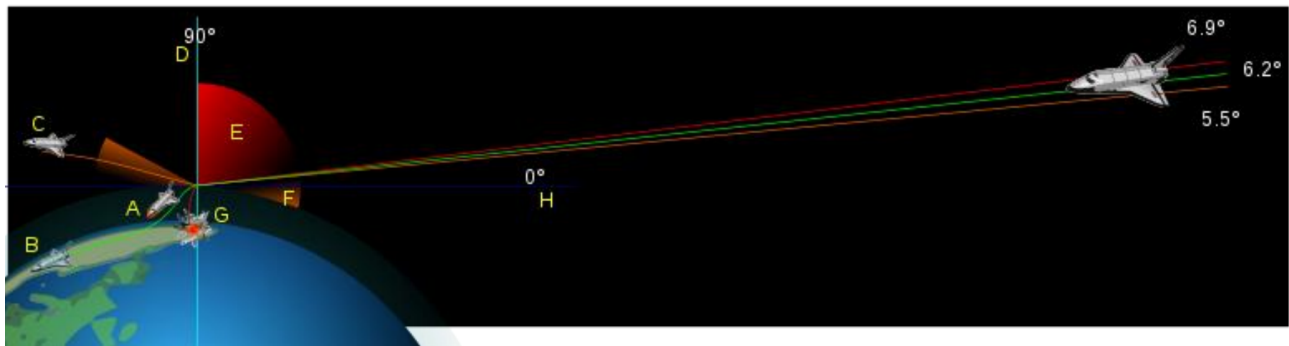


Figure 2.17: Idealised re-entry path.

Re-entry window:

- A - friction with air
- B - in air flight
- C - expulsion lower angle
- D - perpendicular to the entry point
- E - excess friction 6.9° to 90°
- F - repulsion of 5.5° or less
- G - explosion friction
- H - plane tangential to the entry point

Karman line

- Earth - 100 km
- Venus - 250 km
- Mars - 80 km

Most objects enter at hypersonic speeds. Alternative on planets with thick atmospheres or strong gravity - Venus, Titan and the gas giants.

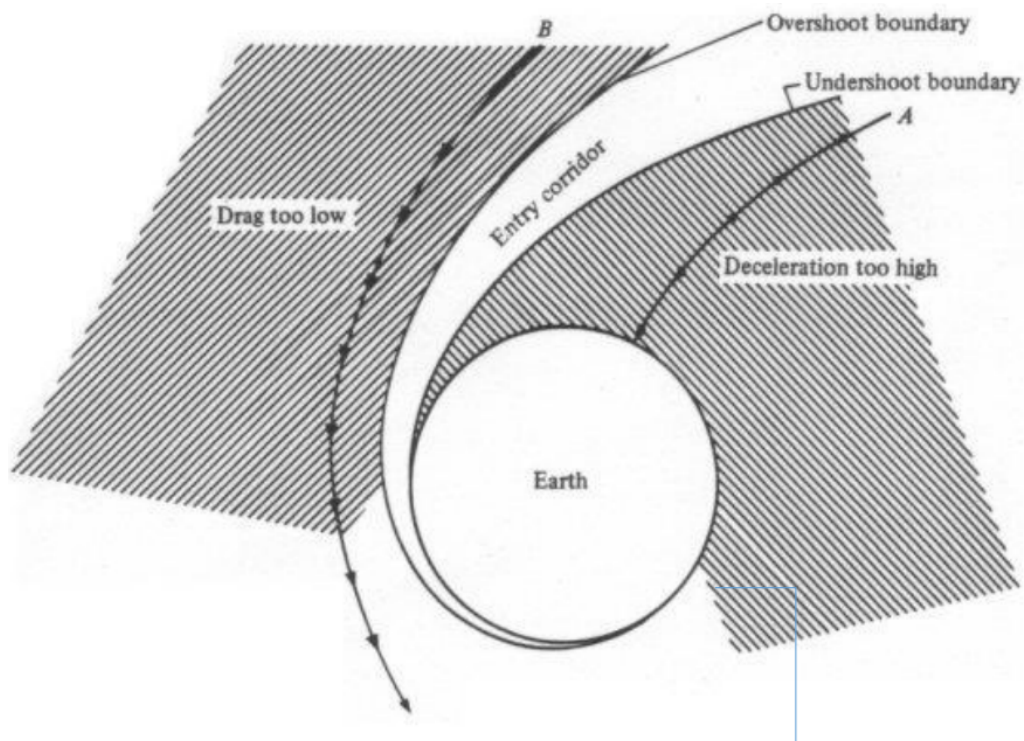


Figure 2.18: Re-entry path for Earth.

2.3.2 Blunt body entry vehicles

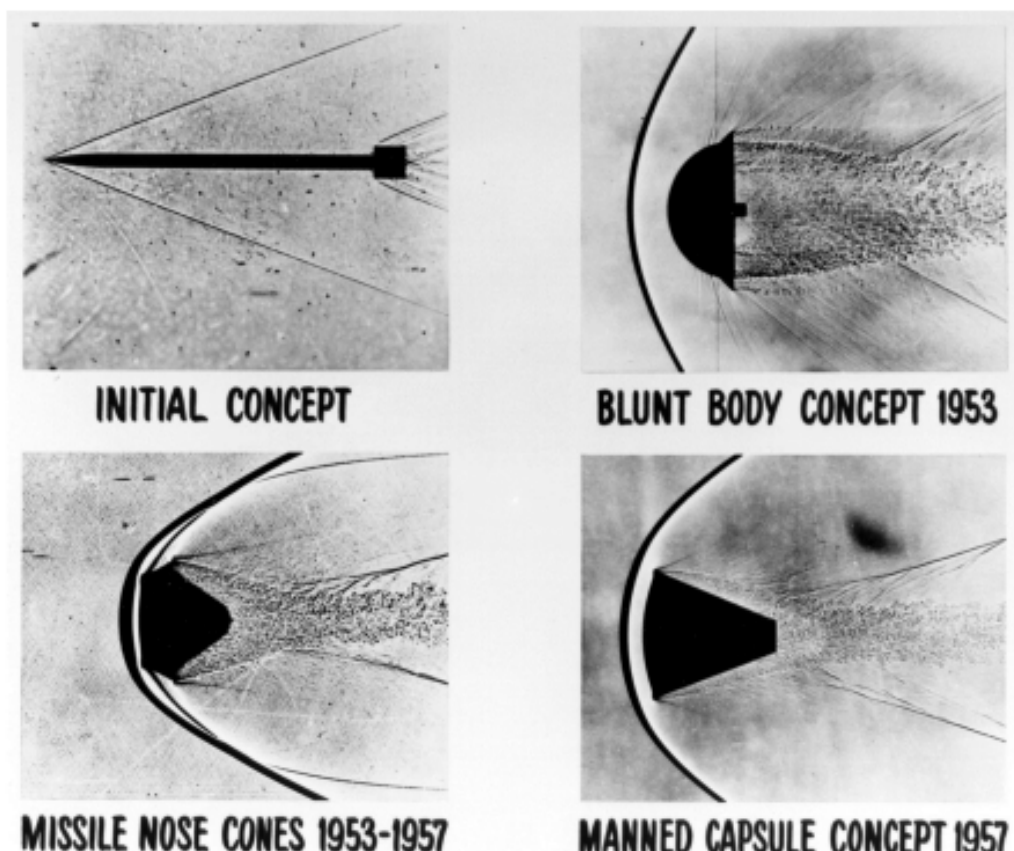


Figure 2.19: Re-entry path for Earth.

Allen & Eggers made the discovery that viscous heating decreases as the inverse square of the drag coefficient.

Shapes of entry types

- Cone



- Biconic



- Lower peak deceleration

Figure 2.20: Shapes of entry path.

2.3.3 Shock layer physics

Perfect gas model - breaks down at 500 K and not useable after 300 K (works okay for Titan because atmosphere is so dense and pressure high). Real gas model - requires table and inclusion of chemistry. Stagnation plane is about 0.14 times nose radius.

2.3.4 Different types of coatings

- SLA-561V stands for super light-weight ablator - used on all NASA mars missions, Starts to ablate at 100 W cm^{-2} but fails for heat fluxes greater than 300 W cm^{-2} . Peak value on Mars is 21 W cm^{-2}
- Phenolic impregnated carbon ablators - carbon fibre impregnated with phenolic resin. Low density with lowest conductivity. Worked well on Apollo mission capsules which entered at 12.4 km s^{-1} . Can withstand 1.2 kW cm^{-2}
- PICA-X - 10 times cheaper to manufacture than PICA
- SIRCA - silicon impregnated reusable ceramic ablators. Can be machined quite accurately.

Ablation layers

Thermal protection systems are used to protect spacecraft in space and during re-entry. Ablative heat shields displace shock and thermal boundary layer away from the wall. Two approaches:

1. Outer surface chars, melts and sublimes
2. Bulk of layer undergoes pyrolysis and expels product gases

The blowing is what displaces the boundary layers. (Note the similarity in last case with gas turbine engines). Pyrolysis can be measured in real time using thermogravimetric analysis, so that ablative performance can be evaluated. Ablation can also provide blockage against radiative heat flux by introduction carbon into the shock layer thus making it optically opaque. Radiative heat flux blockage was the primary thermal protection mechanism of the Galileo Probe TPS material (carbon phenolic). Carbon phenolic was originally developed as a rocket nozzle throat material.

2.3.5 Thermal soak

When pyrolysis does not occur, conductivity increases and heating occurs. All the TPS fail when the heating is reduced. Space Shuttle TPS tiles can withstand 1000 K one side and warm to the touch on the other side, but they are very brittle.

2.3.6 Cooling methods

- Passive - dump the heat shield at the last moment
- Actively cooling by radiating heat - e.g. hypersonic aircraft
- Feathered re-entry
- Inflatable heat shield

2.4 Conclusions

- Fascinating mixture of design and material selection
- Interesting overlap in the physics for both gas turbines and re-entry spacecraft

Chapter 3

Large Spatial and Temporal Variations of Temperature

3.1 Introduction

Many different engineering materials are subject to intense heating and cooling in localised regions. As with our previous discussion about materials, the temperature might be spatially or temporally variable. In Lecture 13, we looked at the thermoelastic response of materials subject to small temperature variations. Their response can be dealt with via a linear elastic model. In this chapter, we look at the effect of a large temperature applied to a material which are sufficient to generate a plastic response and how the spatial and temporal variation affects the material properties.

The incandescent light bulb initially failed due to the thermal fatigue and melting problems. This was largely a material selection and corrosion problem. Turning a light on and off generates enormous thermal stresses, but keeping it on continuously is fine. The filament is made of tungsten which has a high melting point. The inert gases around the filament stop evaporation. Most of energy dissipated is thermal.

Types of heating processes

- **Mechanical heating**, usually by friction
- **Electrical heating**, using the material itself for energy release (e.g. induction heating), or more commonly by external means with an electrical resistance made of Nichrome (60% Ni, 25% Fe, 15% Cr) or Kanthal (70%, 24% Cr, 5% Al)
- **Radiation heating**, either with microwaves, infrared radiation from heated wires protected inside a quartz-glass (wires can be made of tungsten, carbon, Kanthal or Nichrome; naked Nichrome coiled wire was also used in the past), or using visible radiation (with a laser).
- **Chemical heating**, mainly by combustion, but also by hydrogen formation after atomic hydrogen is produced in an electric car, for instance.
- **Nuclear heating**, by nuclear fission or fusion

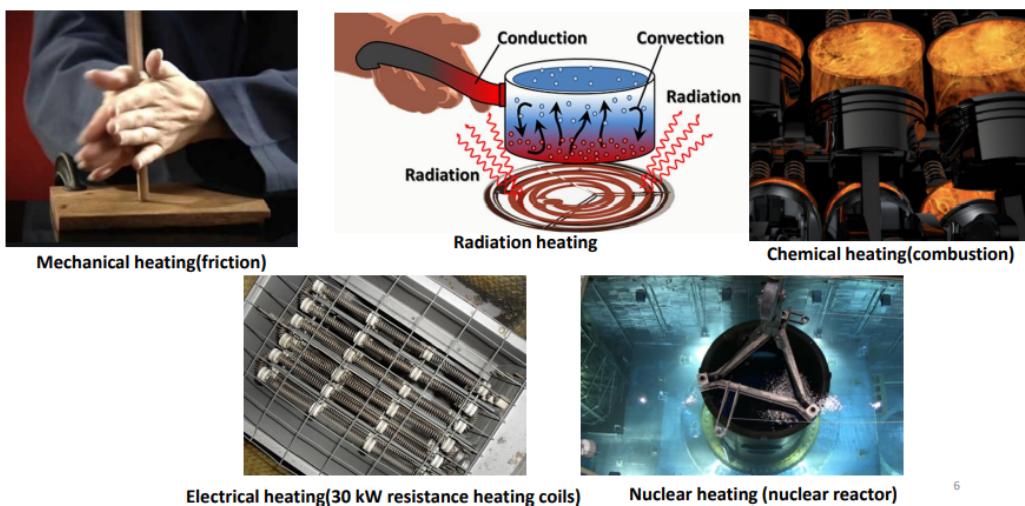


Figure 3.1: Heating processes.

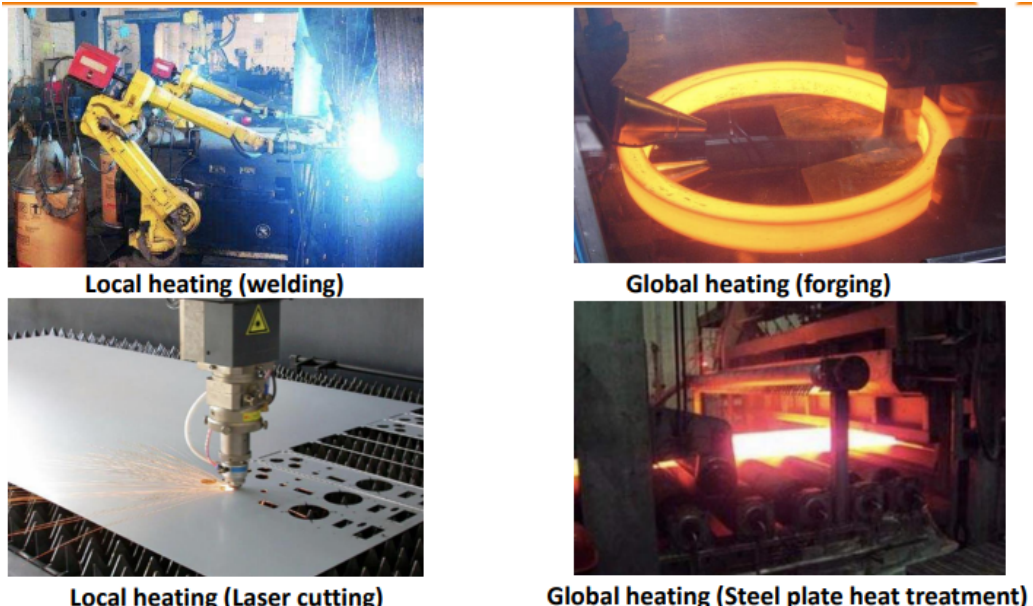


Figure 3.2: Localised heating processes.

3.2 Practical application of heat to a material

Any time a material is heated, the heat is applied spatially and temporally. The characteristics scales have quite different effects on the material and structure.

	Localised	Uniform
Slow	Welding	Heat treatment
Fast	Thermal shocking	Quenching

Table 3.1: Spatial and temporal heat application.

3.2.1 Welding

- TIG - Tungsten gas - electrode is tungsten. You do not need a metal filter. Need a gas tank to protect the weld - most often applied to stainless steels and light metals

- Flux-cored Arc Welding - similar to MIG. Uses a wire to serve as an electrode and a metal filler fed through the wand. Wire has a flux that creates the gas shield. Tends to have slag left so usually needs a clean-up
- Stick (Shielded Metal Arc Welding). Replaceable electrode stick that forms the filler metal. Arc is created at the end of the electrode. Stick is coated in flux that protects the metal from oxidation
- MIG welding (metal inert gas). Filler metal is consumable wire that acts as an electrode
- Laser beam welding - used on a few metals with laser providing the heat
- Plasma Arc Welding - uses a smaller arc with a high pressurised gas that is ionised and electrically conductive

Small amount of molten metal are introduced in the gap between two components to solidify the body. Major regions are:

1. Fusion where the parts of the metal have melted and combined with filler material
2. Heat affected zone - region next to steel that have undergone microstructural changes

3.2.2 Friction welding

<https://www.youtube.com/watch?v=RTEP9QdTn5k>



Figure 3.3: Friction welding.

3.2.3 Radiation heating

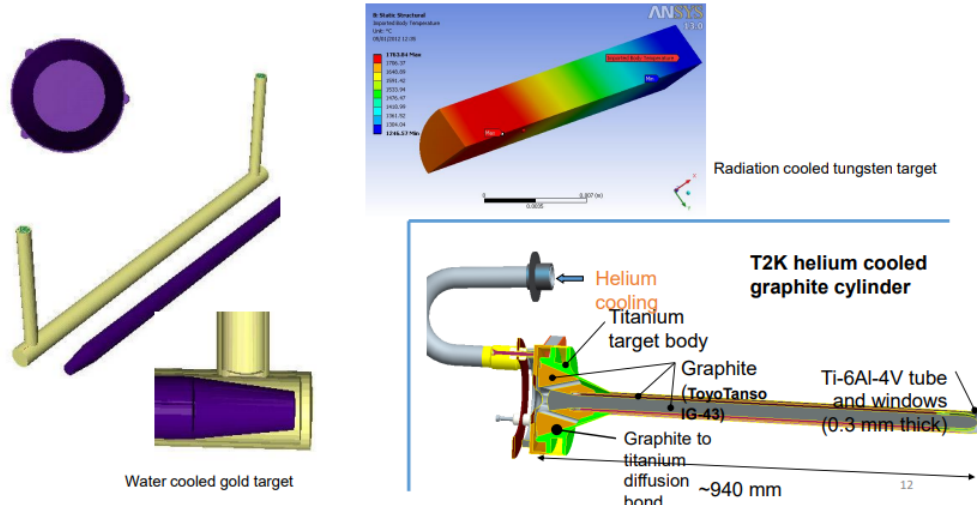


Figure 3.4: Radiation heating.

3.2.4 Laser heating

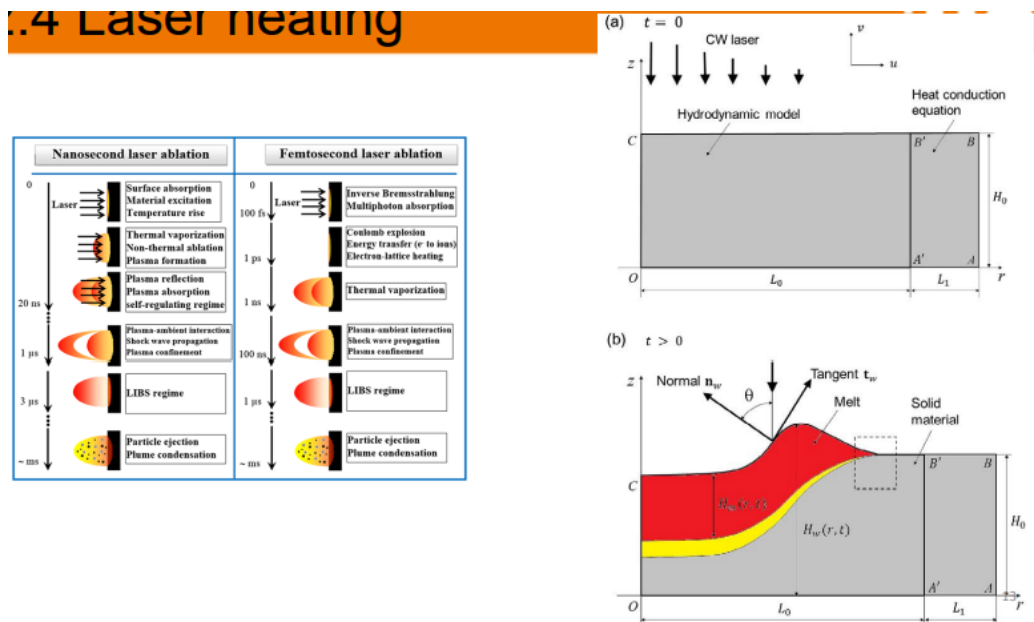


Figure 3.5: Laser heating.

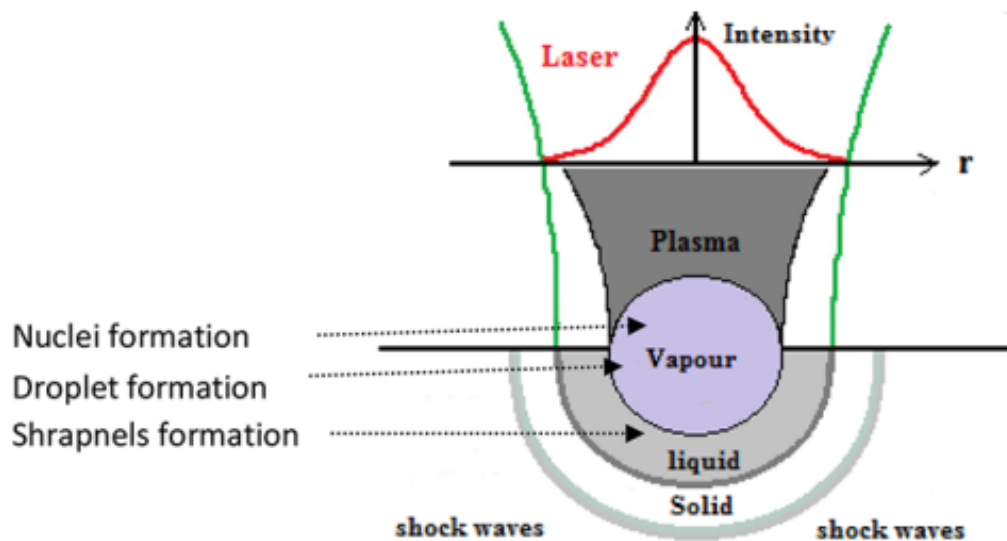


Figure 3.6: Close-up of laser heating.

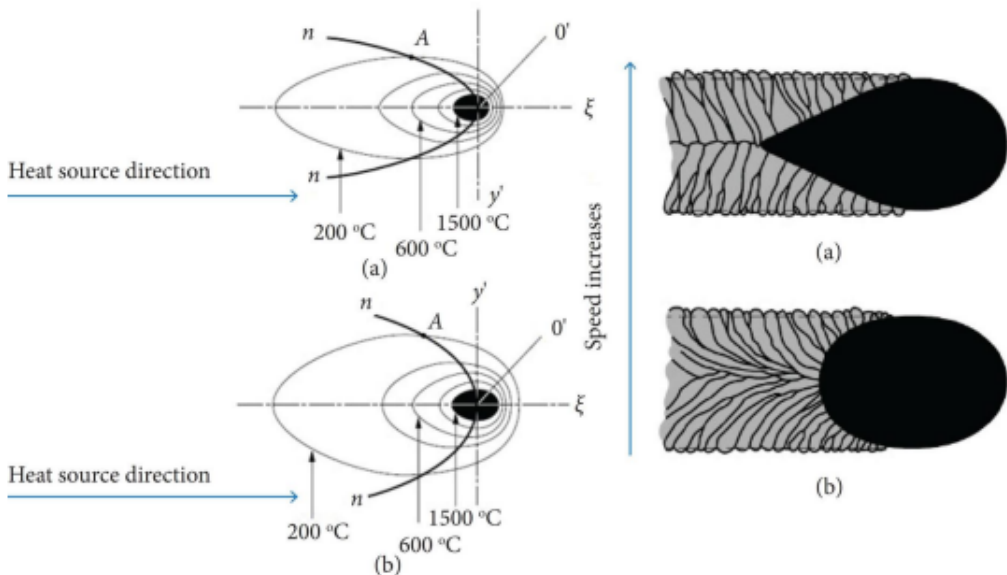


Figure 3.7: Close-up of laser heating.

The heat spreads out through diffusion from a moving source. The temperature distribution can be analysed using simple mathematical models of a moving source and this is discussed in Worksheet 15.

3.3 Structural changes in the matter

https://www.youtube.com/watch?v=uG35D_euM-0&authuser=0

3.3.1 Microstructural changes

Metals are comprised of a symmetrical structure of atoms known as an allotrope. Heating the metal will displace atoms from their position and the displaced atoms form a new structure. This process is known as allotropic phase transformation. Allotropic phase transformation alters the hardness, strength and ductility of the metal. The most important allotropic phase transformation is undergone by iron. When iron is heated past 912 °C it is able to absorb more carbon which is essential for the manufacture of stainless steel.

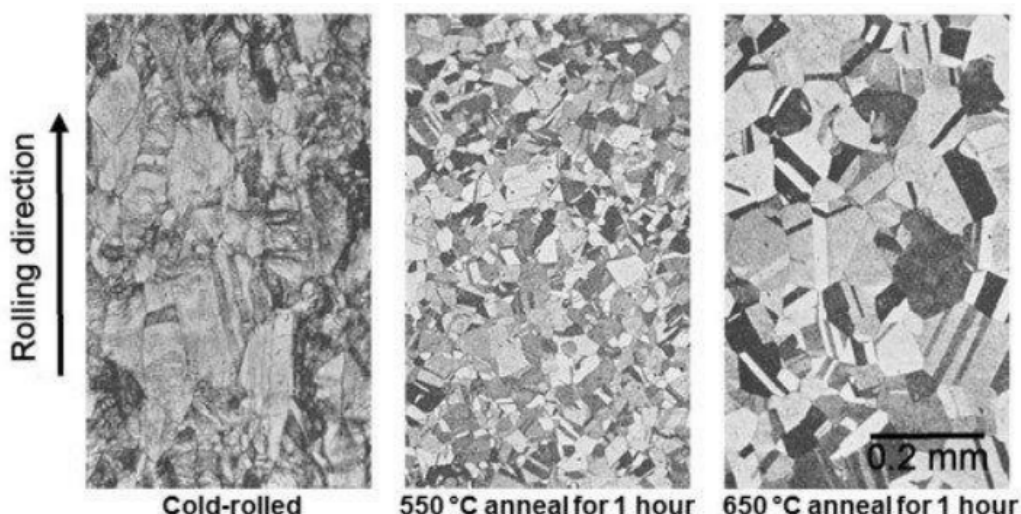


Figure 3.8: Effect on microstructure from cold rolling and then annealing.

Heat treatment

Annealing is used to soften metals including iron, steel, copper, brass and silver. The process involves heating the metal to a specific temperature then allowing it to cool slowly at a controlled rate. Annealing alters the physical and chemical properties of the metal to increase ductility and reduce hardness. This facilitates shaping, stamping or forming processes, and allows the metal to be cut more easily. Annealing also enhances electrical conductivity.

Normalising is applied to alloys to provide uniformity in grain size and composition. The metal is heated to a predefined temperature then cooled by air. The resulting metal is free of undesirable impurities and exhibits greater strength and hardness. Normalising is often used to produce a harder and stronger steel, albeit one that is less ductile than that produced by annealing. Typically, the normalising process is performed on materials that will be subjected to machining, because the process has improved this attribute.

Hardening is applied to steel and other alloys to improve their mechanical properties. During hardening, the metal is heated at a high temperature and this temperature is maintained until a proportion of carbon has been dissolved. Next the metal will be quenched, which involves rapidly cooling it in oil or water. Hardening will produce an alloy which has high strength and wear resistance. However, hardening will also increase brittleness and is not suitable for engineering applications. When there is a need to have the surface of the component hard enough to resist wear and erosion, while maintaining ductility and toughness to withstand impact and shock loading - surface hardening would be used.

Tempering is applied to steel where ductility is desired. Untempered steel is very hard but too brittle for most practical applications. Tempering is a low temperature heat treatment process normally performed after hardening (neutral hardening, double hardening, atmospheric carburising, carbonitriding, or induction hardening) in order to reach a desired hardness/toughness ratio. The process involves heating steel to a lower temperature to reduce some of the excess hardness. The metal is then allowed to cool in still air which results in a tougher and less brittle steel.

3.3.2 Macroscopic changes

Large temperature variations lead to inelastic and non-recoverable deformations. For plastic deformation require about 0.2% residual strain. Since the strain generated a temperature difference of ΔT scales as $\epsilon \sim \Delta T \alpha$. With a typical value of $\alpha \sim 1 \times 10^{-5} \text{ K}^{-1}$, we only need $\Delta T \sim 200 \text{ K}$ to generate this strain. Large temperatures leads to melting, rearrangement of bonds and this is what is used in casting and welding. Ductile and malleable materials can absorb changes while brittle materials fracture.

3.4 Soldering, brazing, welding

- Soldering is a low-temperature process ($60\text{-}400^\circ\text{C}$) that uses a low-melting metal (a base of tin combined with lead, silver, antimony, bismuth, indium) to join similar or dissimilar metals; it is mainly used in electronic boards
- Brazing is a mid-temperature process ($450\text{-}1200^\circ\text{C}$) that uses a high-melting metal (a base of silver combined with nickel, copper, zinc) to join similar or dissimilar metals; it is mainly used in copper piping and jewellery
- Welding is a high temperature process ($800\text{-}2000^\circ\text{C}$) that uses a powerful heat source to locally melt and join similar metals; it is mainly used in iron and steel work

Influence of localised heating

Close to the weld there is a heat affected region where the microstructure is affected by the heat. The metal in this area is generally weaker than the base material and the fusion zone. This is where the residual stresses are found.

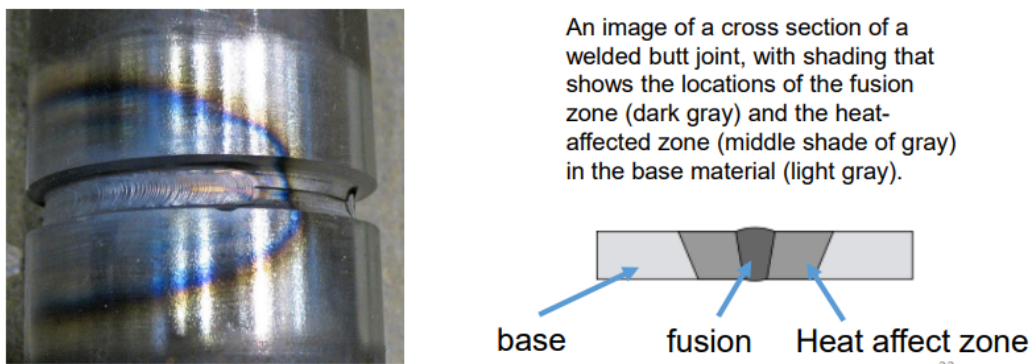


Figure 3.9: Influence of localised heating on a weld.

Heat affected zone

This is the ring that surrounds the weld which affects the alloy. If thermal diffusivity is high, cooling rate is high so the HAZ is smaller. If thermal diffusivity is low, cooling rate is low so the HAZ is bigger. Other measures are used, such as rate of heat input for weld where:

$$Q = \frac{60VI}{1000U} \times \text{efficiency} \quad (3.1)$$

- Q is the heat input (kJ mm^{-1})
- VI is the electrical power
- U is the speed of the weld

Usually we need $Q \approx 10 - 25 \text{ kJ mm}^{-1}$.

Weld	Efficiency
PAW	0.46
GTAW	0.65
Gas metal arc	0.83

Table 3.2: Welding efficiencies.

Thermoplastic shrinkage

When a plate is heated, there is an elastic convex deformation that fades as it is cooled and a plastic concave deformation. This is exploited in ship manufacturing techniques to create curved sheets.

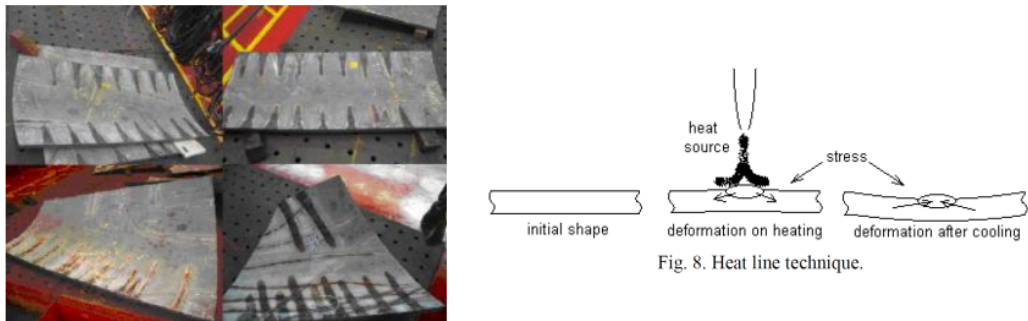


Figure 3.10: Thermoplastic shrinkage.

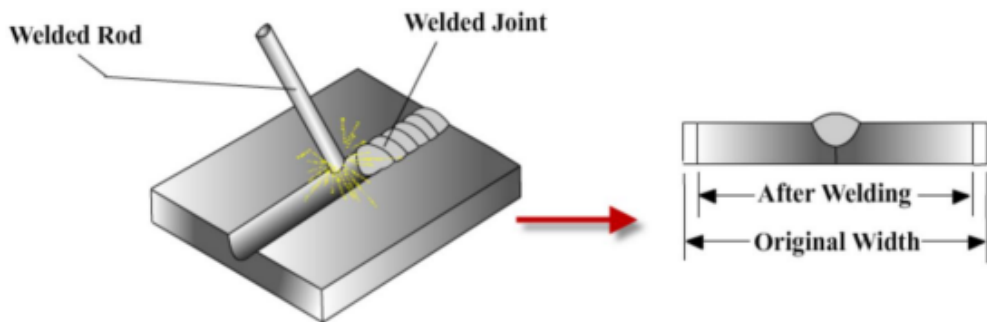


Figure 3.11: Weld shrinkage.

Weld shrinkage - generated by localised stresses caused by heating and distortion of the heated material. Usually leads to transverse and longitudinal shrinkage.

Process of plate heating

The process is known as heat line technique or line heating method of plate bending; it is applied mainly to mild-steel plates, and was started in the 1970s in shipbuilding. It consists of the following steps.

1. Initial heating. It forces the heated mass to expand against the rest of the material, creating great stresses and a very small convex elastic deformation due to the temperature gradient
2. High heating. Up to 1200 K (but usually limited to <995 K to avoid the mild-steel phase transition). It lowers the strength of the heated mass so much, that plastic-yield takes place, that the side material forces the heated mass to bulge in the hottest region
3. After cooling. Forced cooling (usually by water) increases the temperature gradient that forces the heated mass to recover its original strength but not its original shape, because the plastic deformation is not reversible, causing a shrinkage that pulls in from the rest of the material (i.e. in the whole it is not a thermal push but a thermal pull), causing a concave bending (and perhaps some cracks), and minor in-plane deformations due to the point-wise application (instead of the whole line at a time).

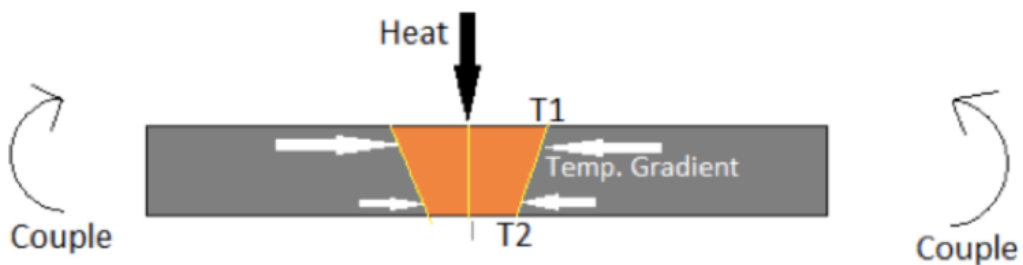


Figure 3.12: Plate heating.

3.5 Rapid changes in temperature

When a material is cooled or heated very rapidly over a small region, thermal stresses can be generated. This occurs due to uneven heating/cooling. Assume top thin layer is rapidly cooled from T₁ to T₂, the stress generated is:

$$\sigma = -E\alpha(T_1 - T_2) \quad (3.2)$$

The rate of heating is characterised by the Biot number,

$$Bi = \frac{hH}{k} \quad (3.3)$$

In contrast to small temperature changes, a hot shock is not the same as a cold shock since the highest stress occurs in different locations. Rapid cooling and heating is used to generate a stress in safety glass that causes it to fracture catastrophically (and safely).

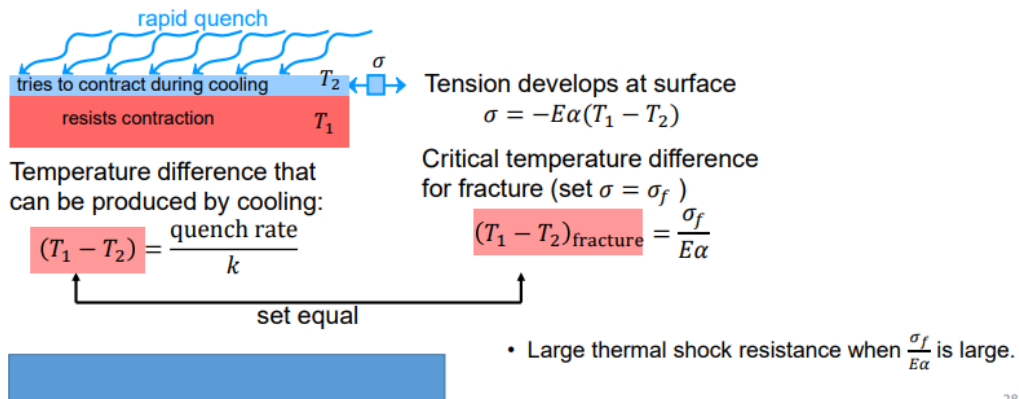
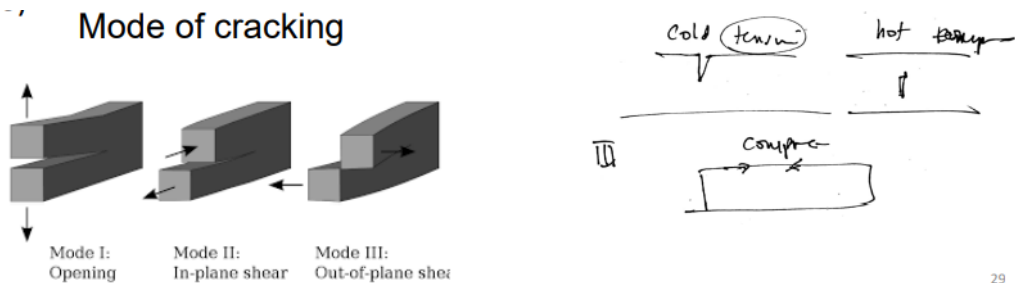


Figure 3.13: Rapid changes in temperature characterised.

3.5.1 Thermal shock

Thermal shock occurs when a thermal gradient causes different parts of an object to expand by different amounts. This differential expansion can be understood in terms of stress or of strain, equivalently. At some point, this stress can exceed the strength of the material, causing a crack to form. If nothing stops this crack from propagating through the material, it will cause the object's structure to fail (read Lu & Fleck 1998).



29

Figure 3.14: Thermal shock.

3.5.2 Stress criterion

The usual measure is the thermal shock resistance parameter:

$$TSR = \frac{\sigma_f k}{E\alpha} \quad (3.4)$$

where:

- σ_f is fracture strength of a material
- α is the expansivity
- k is the thermal conductivity of material
- E is Young's modulus of elasticity

When $TSR >$ critical value, there is a failure. The stress distribution in a thin sheet is:

$$\sigma_{xx} = -E\alpha(T - T_i) + \frac{E\alpha}{2H} \int_{-H}^H (T - T_i) dz \quad (3.5)$$

Kingery (1995) derived two relations.

$$R = \frac{\sigma_f(1-v)}{E\alpha} \quad (3.6)$$

Useful for instantaneous change in surface temperature (infinite h).

$$R' = \frac{\sigma_f(1-v)k}{E\alpha} \quad (3.7)$$

Relatively low Biot modulus. For constant heating:

$$R' = \frac{\sigma_f(1-v)a}{E\alpha} \quad (3.8)$$

Where a is the thermal diffusivity.

3.5.3 Strain criterion

One way to look at for brittle materials is to define:

$$\theta = \frac{\epsilon_c}{\alpha} \quad (3.9)$$

where ϵ_c is the critical strain for failure. This is appropriate for a uniform temperature and high conductivity. If this is not available, then we would use:

$$\epsilon_c = \frac{\sigma_u}{E} \quad (3.10)$$

Reducing failure from shocking

Failure due to thermal shock can be prevented by reducing the thermal gradient seen by the object, by changing its temperature more slowly or increasing the material's thermal conductivity (k).

- Reducing the material's coefficient of thermal expansion (α)
- Increasing its strength (σ_f)
- Introducing built-in compressive stress, as for example in tempered glass
- Decreasing its Young's modulus (E)
- Increasing its toughness, by crack tip blunting (i.e., plasticity or phase transformation) or crack deflection (smaller cracks)

3.5.4 Fraction criterion

Hasselman (1969) developed a unified theory of thermal shock for brittle ceramics. It was 'unified' in the sense that the conditions for the fracture initiation were combined with a consideration of crack propagation. For an infinitely fast quench, from a higher temperature, a thermal stress, σ_{TS} , is generated in the ceramic and is given by:

$$\sigma_{TS} = \frac{\alpha E \Delta T}{(1 - 2v)} \quad (3.11)$$

where E is the Young's modulus, ΔT is the difference in temperature between the initial temperature of the ceramic and the quenching medium, α is the coefficient of linear thermal expansion and v is the Poisson's ratio.

Mechanical model is based on an energy argument. For Griffith microcracks (N per unit volume), spread uniformly in the material,

$$W_t = \frac{3(\alpha \Delta T)^2 E}{2(1 - 2v)} \left(1 + \frac{16(1 - v^2) N l^3}{9(1 - 2v)} \right)^{-1} + 2\pi N l^2 G \quad (3.12)$$

where l is the crack length and $2\pi N l^2 G$ is the energy associated with circular crack of radius l . According to Griffith, the limit of the cracks that are unstable are those where:

$$\frac{dW_t}{dl} = 0 \quad (3.13)$$

Energy of a crack is:

$$\int \sigma d\epsilon = \frac{3\sigma^2}{2\epsilon} \quad \epsilon = \alpha \Delta T \quad (3.14)$$

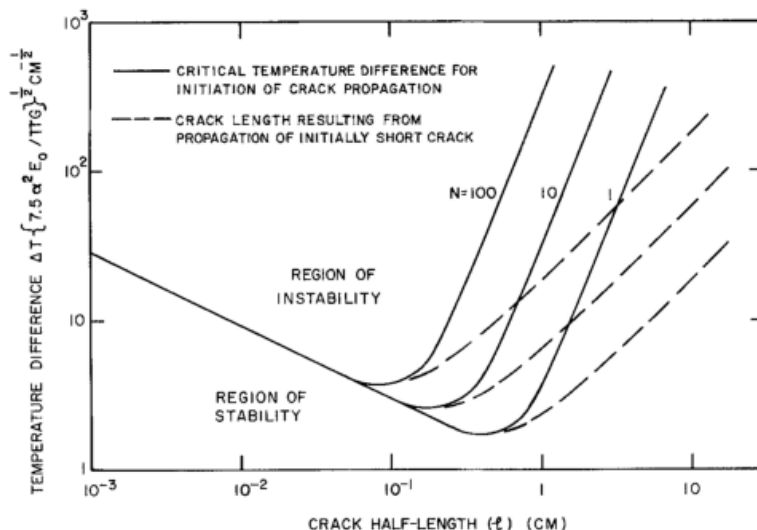


Figure 3.15: Crack lengths against temperature difference.

For short cracks:

$$\Delta T_c = \sqrt{\frac{\pi G (1 - 2v)^2}{2E_0 \alpha^2 (1 - v^2) l}} \quad (3.15)$$

For long cracks:

$$\Delta T_c = \sqrt{\frac{128\pi G (1 - v^2) N^2 l^5}{81\alpha^2 E_0}} \quad (3.16)$$

The results can be expressed in terms of the critical fracture stress:

$$S_t = \sqrt{\frac{GE_0}{2l_0 (1 - v^2)}} \quad (3.17)$$

The dimensionless group is:

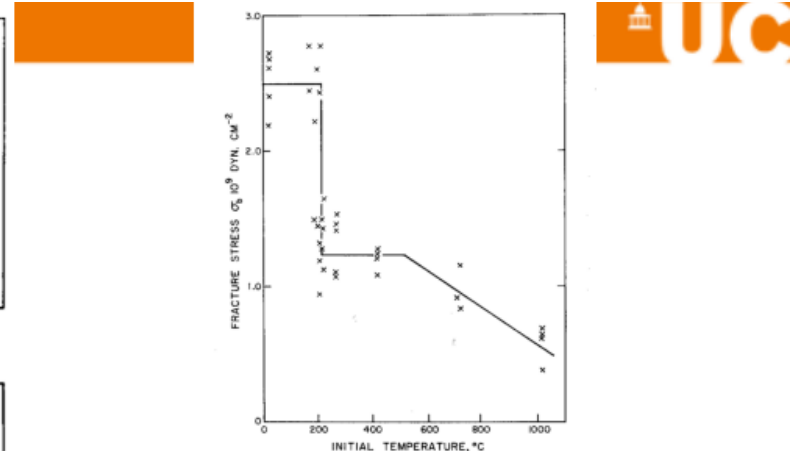
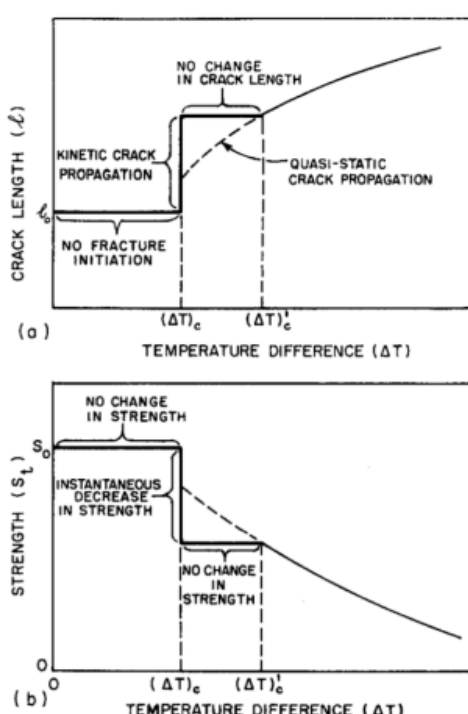
$$\frac{S_t}{\sqrt{GE}} \quad (3.18)$$

The temperature difference inside the material is:

$$\Delta T_i \sim \Delta T \frac{k}{ah} \quad (3.19)$$

Then:

$$\frac{\alpha \Delta T E k \sqrt{l}}{h a \sqrt{\pi G E}} \sim 1 \quad (3.20)$$



Strength at room temperature of 5mm diameter alumina rod subjected to thermal shock by quenching.

Below critical value, no change in crack length. Above critical value, fracture initiated and grow to another length. Hence a jump in the fracture strength.

38

Figure 3.16: Crack lengths , temperature difference, strength and fracture stress.

3.5.5 Material selection

Among the best thermomechanical materials, there are alumina, zirconia, tungsten alloys, silicon nitride, silicon carbide, boron carbide, and some stainless steels. Reinforced carbon-carbon is extremely resistant to thermal shock, due to graphite's extremely high thermal conductivity and low expansion coefficient, the high strength of carbon fibre and a reasonable ability to deflect cracks within the structure.

3.6 Conclusions

The influence of large changes in temperature can be exploited to change the properties of materials and as part of a manufacturing process. In some instances, sudden changes in temperature, can lead to failure either through a yield, strain or cracking. There are approximate models of these processes.

Chapter 4

Low temperature environments

4.1 Introduction

- Low temperature: -273°C , -150°C
- Mechanical challenges - rapid heating / increasing gas pressure
 - Failure / fatigue
- Most low temperature - rise at atmospheric pressure
 - Small volumes
- Through design - challenge becomes managing the thermal component not the mechanical
- Health & Safety - dense / cold gas moves quickly and can suffocate people

Gas	Freezing temperature
CO ₂	-78.5°C (sublimates)
Nitrogen	-196°C
LNG	-161.5°C

Table 4.1: Freezing temperatures of various gases.

The energy density of LNG is comparable to propane and ethanol but is only 60 percent that of diesel and 70 percent that of gasoline.



Figure 4.1: LNG carrier.

An LNG carrier is a tank ship designed for transporting liquefied natural gas. At the end of 2016, the global LNG shipping fleet consisted of 439 vessels. Majority of ships have a capacity of 120 000-140 000 m³.

Alloy	TYPE	APPLICATION
9Ni	9% Ni steel	Storage tanks
304L	Stainless steel type AISI 304L	Piping; Small vessels. Some designs of large storage tanks.
36NiFe	Low expansion, 36%Ni-Fe alloy	Some large storage tank designs. Piping in critical applications.
Al	Aluminium alloy type 5083 (Al-4.5%Mg) Alloy 5154 (Al-3.5%Mg) Alloy 6000 (Al-Si)	Spherical or prismatic storage tanks for ship transportation of LNG. Tubing for the main cryogenic heat exchanger. Forgings such as flanges.

Property	T °C	9%Ni Steel	AISI 304L Stainless Steel	36% Ni Fe Alloy	Al alloy 5083
Density, kg/m ³		7860	7900	8120	2660
Elastic Modulus E, GPa	+20 -196	186 207	193 205	148 138	70 81
Thermal Conductivity, W/m°C	+20 -196	28.5 13.0	13.4-15.1 9	10.5 5.7	117
Mean Coefficient of thermal expansion, α , 10 ⁻⁶ /°C	0 to -196	9.5	14.4 – 15 (at 0°C) 11.7 - 13.5 (at -196°C)	1.5	17.5
Theoretical thermal stress in contracting a rigid length from 0 to -163°C, MPa $\sigma = E\epsilon = E \alpha \Delta T = 163 E \alpha$		304	440	34	228
Theoretical thermal stress in contracting a rigid length from 0 to -163°C, MPa as a percentage of yield strength		51-69%	176%	12.6%	157%

Table 4.2: Tables to show material properties of storage tanks.

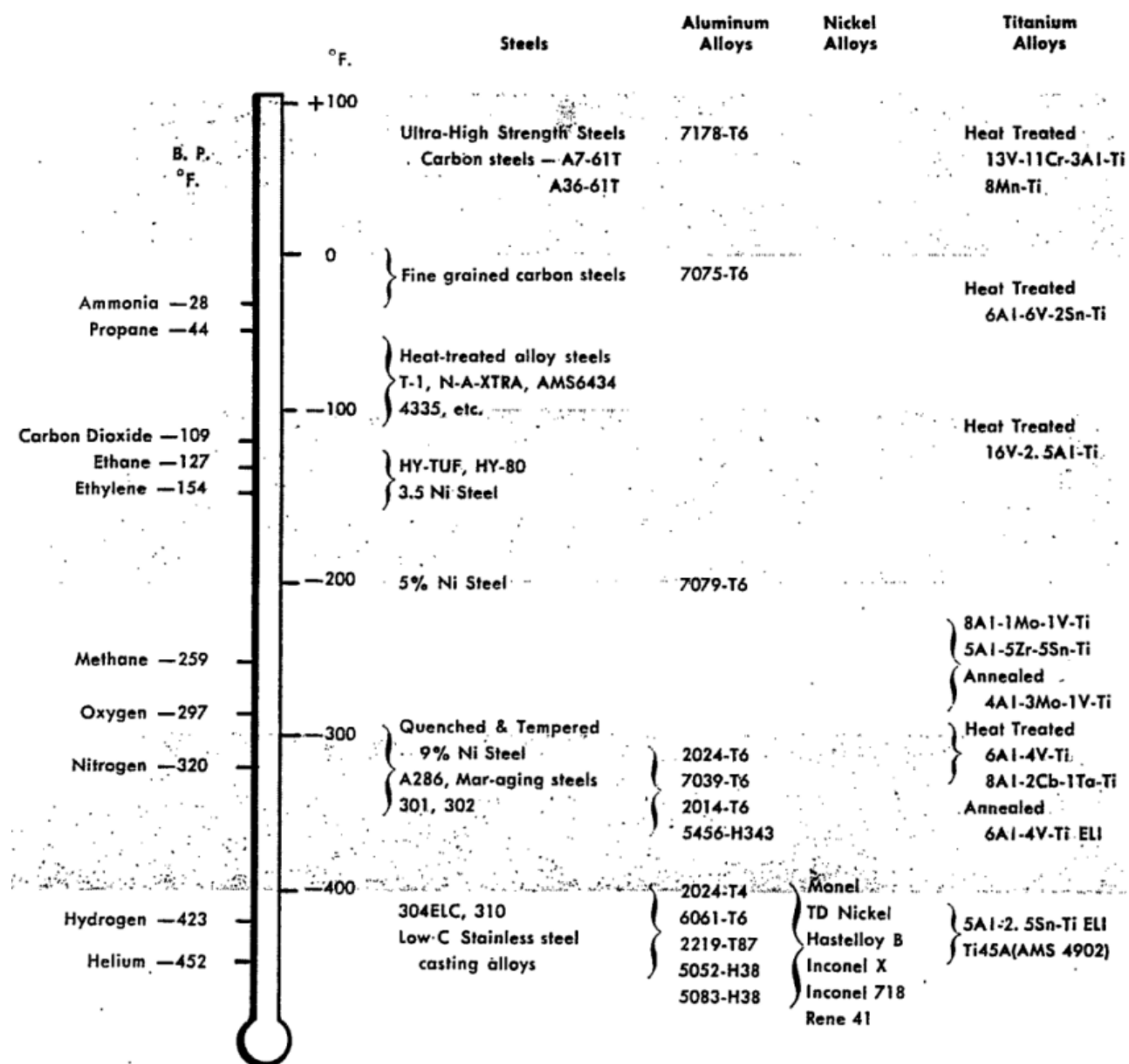


Table 4.3: Table to show materials used to store different low temperature materials.

4.2 Engineering applications

4.2.1 LNG - liquefied natural gas

Methane, CH₄ (with some ethane). 1/6000th the volume of natural gas in the gaseous state (at standard condition for temperature and pressure). It is odourless, colourless, non-toxic and non-corrosive. Hazards include flammability after vaporisation into a gaseous state, freezing and asphyxia. The liquefaction process involves removal of certain components, such as dust, acid gases, helium, water and heavy hydrocarbons, which could cause difficulty downstream. The natural gas is then condensed into a liquid at close to atmospheric pressure by cooling it to approximately -162 °C. Maximum transport pressure is set at around 25 kPa.

4.2.2 Cryogenic transport

Transfer lines are a form of cryostat. Used to transport cryogenic fluids between cryogenic devices. Simplest form is a vacuum jacketed pipe connecting two flasks. Heat is absorbed by the liquid (nitrogen) and as the pipe gets longer, more heating occurs and more vapour generated (which is lost). Higher pressure differential, more heating occurs. The most important design elements are:

- Geometry
- Mass flow rate
- Temperature and pressure change
- Cryogenic fluid
- Mechanical properties of the materials

4.3 Thermal bowing

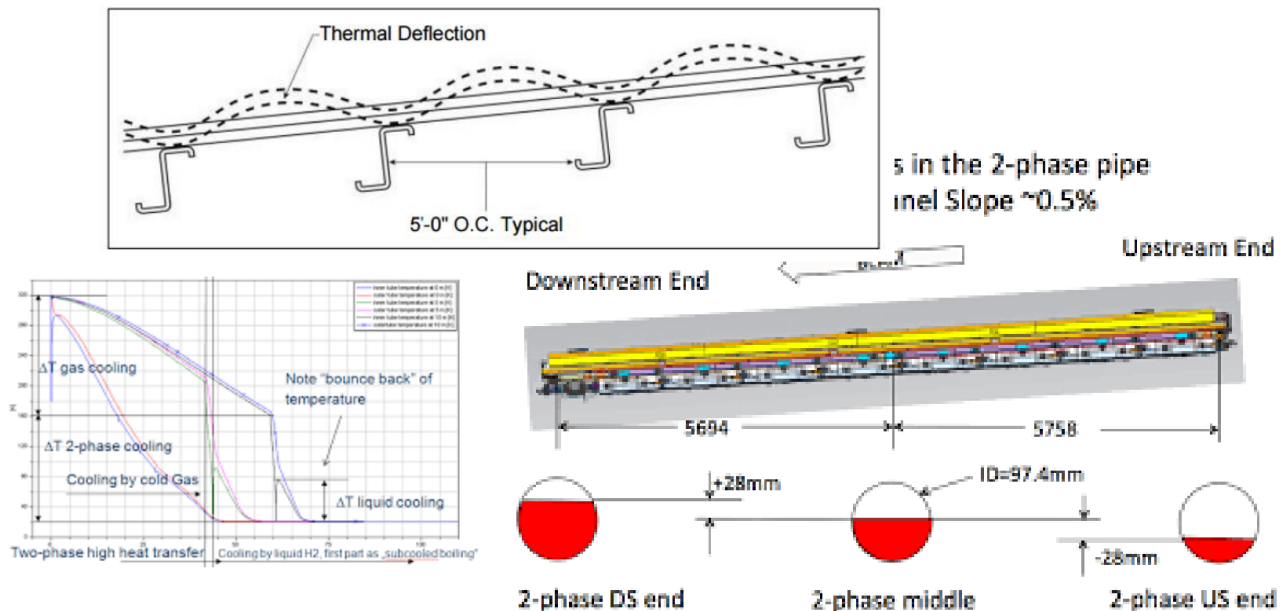


Figure 4.2: Thermal bowing.

Laterial variation of temperature

Thermal bowing occurs due to two processes:

1. Restrained thermal expansion
2. Temperature gradient across pipe

Assuming no mean temperature increase:

$$\Delta T = 0 \quad (4.1)$$

Thermal Bowing with ends restrained against rotation

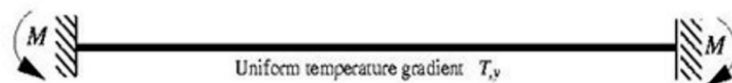


Figure 4.3: Fixed end beam subjected to a uniform thermal gradient.

Uniform moment over the length:

$$M = EI\phi = EI\alpha T_{y} \quad (4.2)$$

Thermal Bowing with ends restrained against translation

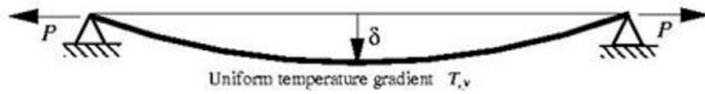


Figure 4.4: Laterally restrained beam subjected to a uniform thermal gradient.

A tensile force P will be generated causing a tensile $P - \delta$ moment Py over the length of the beam,

$$\frac{d^2y}{dx^2} = \phi + \frac{Py}{EI} \quad (4.3)$$

or

$$\frac{d^2y}{dx^2} - k^2y = \phi \quad (4.4)$$

where,

$$K = \sqrt{\frac{P}{EI}} \quad (4.5)$$

The solution of this equation is,

$$y(x) = -\frac{\phi}{k^2} \left(\frac{\cosh(kl) - 1}{\sinh(kl)} \sinh(kx) \cosh(kx) + 1 \right) \quad (4.6)$$

Derivation

The derivation starts with the point that the displacement is:

$$u = f(x) + yf_1(x) + zf_2(x) \quad (4.7)$$

The longitudinal strain is

$$\epsilon_{xx} = \frac{\partial u}{\partial x} = f'(x) + yf'_1(x) + zf'_2(x) \quad (4.8)$$

The stress field is

$$\sigma_{xx} = E(\epsilon_{xx} - \alpha T) \quad (4.9)$$

The equilibrium constraints are

$$\int \sigma dA = 0 \quad (4.10)$$

$$\int \sigma y dA = 0 \quad (4.11)$$

$$\int \sigma z dA = 0 \quad (4.12)$$

The geometrical constraint is

$$\int y dA = \int z dA = 0 \quad (4.13)$$

Cross-pipe variation of temperature:

$$\sigma_{xx} = -\alpha E(T - \bar{T}) + \frac{I_y M_{Tz} - I_{yx} M_{Ty}}{I_y I_z - I_{yz}^2} y + \frac{I_y M_{Tz} - I_{yx} M_{Ty}}{I_y I_z - I_{yz}^2} z \quad (4.14)$$

where

$$I_z = \int y^2 dA \quad (4.15)$$

$$I_y = \int z^2 dA \quad (4.16)$$

$$I_{yz} = \int yz dA \quad (4.17)$$

$$M_{Ty} = \int \alpha ETz dA \quad (4.18)$$

$$M_{Tz} = \int \alpha ETy dA \quad (4.19)$$

For a pipe

$$\sigma_{xx} = -\alpha E (T - \bar{T}) + \frac{M_{Tz}}{I_y} y \quad (4.20)$$

For the lateral displacement

$$\frac{d^2 v}{dx^2} = -\frac{M_{Tz}}{EI_z} \quad (4.21)$$

$$\frac{d}{dx^2} \left(EI_z \frac{d^2 v}{dx^2} \right) + \frac{d^2 M_{Tz}}{dx^2} = F \quad (4.22)$$

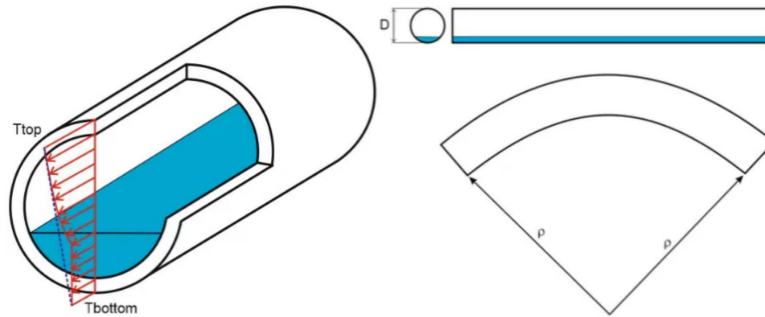


Figure 4.5: Cross-section of pipe.